SAE INTERNATIONAL

ARTICLE INFO
Article ID: 03-18-02-0016

doi:10.4271/03-18-02-0016

Real-World Vehicle Estimation and Control of Indirect Emissions Control and Performance Evaluation of Electric Vehicles with In-Wheel Motors

Mohamed S. Shiba,[1] Shawki A. Abouel-Seoud,[2] W. Aboelsoud,[3] and Ahmed S. Abdallah[2]

[1]October University for Modern Sciences and Arts (MSA), Mechatronics Systems Engineering Department, Faculty of Engineering, Egypt
[2]Helwan University, Faculty of Engineering (Mataria), Egypt
[3]Ain Shams University, Mechanical Power Engineering Department, Faculty of Engineering, Egypt

Abstract

The growing number of automobiles on the road has raised awareness about environmental sustainability and transportation alternatives, sparking ideas about future transportation. Few short-term alternatives meet consumer needs and enable mass production. Because they do not accurately reflect real-world driving. Current models are unable to estimate vehicle emissions. However, the purpose of this research is to present an application of an adaptive neuro-fuzzy inference system for managing the various factors contributing to vehicle gasoline engine exhaust emissions. It examines how well the three known standardized driving cycles (DSCs). Accurately reflect real-world driving and evaluate the impact of real-world driving on vehicle emissions. Indirect emissions are inversely proportional to the vehicle's fuel consumption. The methodology used is Eco-score methodology to calculate indirect emissions of light vehicles. Expected emission charge estimates for different using styles. Emission rates range substantially between battery classes. The vehicle's gasoline efficiency is four times better than a similar automobile, but neither mass nor charge multiplied appreciably. The range of this car is not restrained by the battery length, which increases driver comfort, while automobile meets customer expectations in addition to environmental worries and advantages. Despite the fact that they continue to be affordable, they offer a possibility for mass manufacturing reducing overall environmental effects. In keeping with the consequences, the adaptive neuro-fuzzy inference system works nicely to simulate and regulate vehicle engine exhaust emissions.

However, the final objective of a regulatory-oriented studies software that focuses on air pollution from mobile sources is to identify and quantify any outcomes that the emissions may have on human fitness.

However, before we invest highbrow and economic sources, we need to first recognize the restrictions of modern information and methodologies that preclude accurate estimates of risk to human health. Destiny research packages should be justified by way of their promise to triumph over these boundaries. The goal of this extent, then, is to identify troubles and pick out a studies schedule with a purpose to be only in advancing our potential to quantify the fitness dangers related to air pollution.

History

Received: 31 May 2024
Revised: 05 Nov 2024
Accepted: 26 Feb 2025
e-Available: 17 Mar 2025

Keywords

Electric vehicle, Fuel consumption, Energy consumption, Indirect emissions, ECE 15 (urban driving cycle), US06 (city mode driving cycle)

Citation

Shiba, M., Abouel-Seoud, S., Aboelsoud, W., and Abdallah, A., "Real-World Vehicle Estimation and Control of Indirect Emissions Control and Performance Evaluation of Electric Vehicles with In-Wheel Motors," *SAE Int. J. Engines* 18(2):2025, doi:10.4271/03-18-02-0016.

ISSN: 1946-3936
e-ISSN: 1946-3944

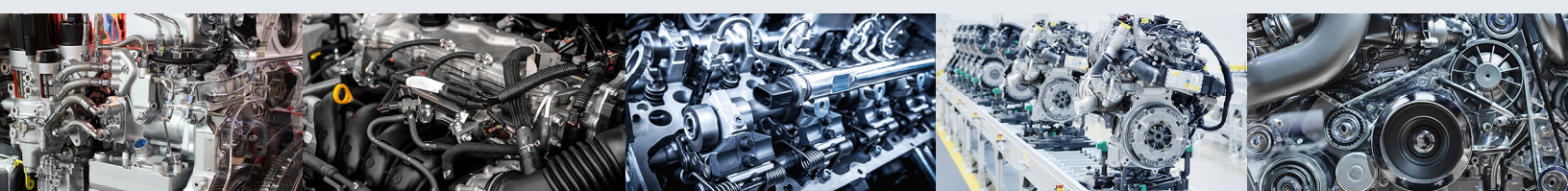

1. Introduction

The industry of automotive is making constant attempts to reduce its overall environmental impact on carbon dioxide (CO_2) emissions, one of the main greenhouse gases. Since battery electric vehicles (BEVs) produce far less pollution than traditional internal combustion engine vehicles (ICEVs) powered by gasoline or diesel, BEVs are becoming more and more recognized as a technological advance. An in-depth well-to-wheel framework is used in a particular study assessing the effect of ICEVs and BEVs on air pollution, taking into account the full energy flow process from source extraction to vehicle operation. Furthermore, flexible and adaptable manufacturing systems have been created to manage a wide range of products and product families [1].

Product analysis techniques are critical to the design and improvement of production processes as well as the selection of the best product matches. However, it is difficult to assess and choose the optimal product family combinations for production systems because present methodologies frequently concentrate on physically analyzing a particular product or product family. A new methodology has been proposed to assess current goods based on their functional and physical states. Transportation is a prime and unexpectedly developing contributor to greenhouse gasoline emissions, specifically CO_2. Passenger vehicles contribute over 6% to global CO_2 emissions. Electric vehicles (EVs) have received interest as an approach to lessen localized vehicle emissions. But, the examined addresses a gap in studies by thinking about oblique emissions from the energy era needed for EVs. It presents a complete energy device analysis, incorporating indirect emissions of CO, CO_2, NOx, and PM emissions from the power supply of various EV batteries. These techniques consider one-of-a-kind driving patterns (ECE-15 emissions) to evaluate their effect on vehicular emissions, and the results show that adaptive neuro-fuzzy inference scheme (ANFIS) effectively predicts exhaust emissions, with errors between the model predictions and measured values falling within the accepted threshold. Alternatively, it additionally suggests that the statistics reflecting the procedure are healthful but, there are some data factors exceeding the threshold. Those factors look like outliers springing up from the weight temporary periods. However, the schooling of the neural network through the usage of the hairy rule base for selection of proper and best rule is considered in the next segment (designed ANFIS controller).On this prospect, four ANFIS controllers for risky gases such as CO_2, CO, NOx, and overall hydrocarbons (THC) have been demonstrated. When there are no sufficient entire variables, it has been claimed that the ANFIS controller might take the role of the traditional digital controller in a transferring automobile. The ANFIS controller established the predicted overall performance following tests utilizing a complete engine model made to increase popular simulation surroundings and MATLAB. The ANFIS controller has the subsequent blessings over the opposite controllers described within the literature: first, in comparison to a conventional PID controller, it may manage nonlinearity far higher as it directly controls overall performance and exhaust. Second, it avoids the need to calibrate the physical engine models in opposition to the actual devices because it no longer relies on any bodily engine fashions. Subsequently, as it changed into created in real-time surroundings, an actual-time system can without delay use it.

While biofuels were initially considered beneficial for reducing greenhouse gas emissions by sequestering carbon during feedstock growth, recent studies have highlighted overlooked emissions. Converting grassland and forests into new cropland globally, driven by increased biofuel demand, results in carbon emissions. For example, corn-based ethanol can increase greenhouse gases for 167 years due to land-use changes. The study emphasizes the importance of using waste products and raises questions about strict biofuel mandates [2].

Addressing greenhouse gas emissions, particularly CO_2 from the transportation and energy sectors, is a significant environmental concern. The use of electric cars is suggested as a means to reduce emissions, but the extent of reduction depends on electricity generation methods. Research analyzing EVs indirect emissions using real-world data revealed that charging during the afternoon utilized more renewable energy, but the impact was relatively small. Optimization of driving and charging habits, along with reducing the electricity grid's carbon intensity, is crucial for maximizing EVs' environmental benefits [3].

Macro-level transformation pathways are the principle focus of the junction of integrated evaluation (IA) and existence cycle assessment (LCA) modeling, which takes an extensive environmental view. Modern-day IA models, characterized through tension and micro-orientation, complement LCA's historic existence cycle attention. A way has been developed to achieve coefficients from comprehensive LCA to be used in IA models, permitting IA researchers to explore the life-cycle consequences of technological advancements and scenarios. The approach helps the regular software of IA version-specific situation statistics while making use of LCA coefficients, providing insights into the worldwide electricity supply until 2050 [4].

Plug-in electric-powered vehicles (PEVs) are a likely strategy to lower greenhouse gas (GHG) emissions in the transportation quarter, mainly in a mild pointy drop in carbon emissions from the production of strength. Globally, the usage of renewable power assets to generate strength factors to a thorough trade in the quantity of carbon included in electricity used to provide and rate batteries. But the majority of research ignores regional changes in the generating mix and instead assumes that energy has a constant carbon content. Waiting for cleaner PEV battery manufacturing cannot make up for emissions

from combustion vehicle usage, so early PEV market diffusion is the most effective way to use the available carbon budget. Based on short-lived measurements that determine the quality of wheel emissions and future changes in the electricity mix [5].

EVs continue to represent a small fraction of new car purchases, despite the unexpectedly rapid decrease in battery prices, making them more affordable and boosting sales. This unexpected decline in electric car battery costs highlights the unpredictability of battery cost development, influencing the feasibility of transitioning to low-carbon transportation. Integrated assessment models suggest that reducing emissions in the transportation sector is more challenging than in other industries [6]. This study explores the impact of various battery costs and potential changes in climate policy on EV sales. The model indicates that policy incentives' effectiveness is heavily influenced by battery floor costs, as significant EV sales (15% or more) occur only when battery costs drop to $100/kWh or less. Understanding the lower bounds of battery costs, in addition to the rapid rate of cost decline, is crucial for accurately modeling long-term global energy transitions.

The pollution from automobile exhaust pipes might be significantly reduced by means of the great utilization of electrical cars. Analysts warn that this can bring about expanded indirect emissions because transportation regulations do not commonly govern the production of batteries or strength. Capability coverage situations that charge emissions handiest at the tailpipe vs both tailpipe and indirect emissions were analyzed using incorporated strength modeling and life-cycle evaluation [7]. Surprisingly, models accounting for indirect emissions predict higher EVs sales while generating fewer overall emissions. This is attributed to anticipated technological advancements offsetting emissions from electricity and battery production. The study suggests that large-scale adoption of electric cars can reduce CO_2 emissions through multiple channels, benefiting from the ongoing decarburization of the electricity supply and the pricing of carbon from stationary sources.

Greenhouse gas emissions, particularly CO_2 emissions from transportation and energy industries, remain a significant environmental concern. While electric cars are proposed as a solution, their emission reduction depends on the source of electricity used for charging. Real-world data analysis of indirect emissions from electric cars reveals that charging during the day utilizes more renewable energy, but the impact is relatively small due to the vulnerability of renewable sources. The study emphasizes the need to optimize driving and charging habits and reduce the electricity grid's carbon intensity to fully realize the environmental benefits of EVs [3].

LCAs of electric mobility yield conflicting findings, and a study of 44 articles released between 2008 and 2018 reveals challenges in objective definition and modeling choices. The carbon intensity of the electricity mix accounts for 70% of the variation in outcomes, emphasizing the need for a common framework to guide evaluations and policymaking [8].

The development of EVs over the past two decades aimed to reduce harmful emissions and energy consumption in the transportation industry. However, higher manufacturing costs of EVs compared to conventional internal combustion engine vehicles pose a significant hurdle. Cost–benefit evaluations and comprehensive studies struggle to characterize all positive and negative aspects of EVs, prompting questions about their overall efficacy. Existing literature is examined to provide insights into the performance of EVs across environmental, energy, cost, and reliability aspects [9].

Sustainable intensification, addressing rising global food demand while minimizing environmental impact, is a major challenge in the agri-food industry. An input–output model is employed to analyze the entire value chain within a nation, considering the flows along the value chain. The study focuses on Ireland, where agricultural emissions account for nearly 30% of total emissions, examining carbon footprints and pollution sources in specific agri-food value chains [10].

Considering the rapid decrease in carbon emissions from power generation, PEVs emerge as a viable solution for reducing greenhouse gas (GHG) emissions in the transportation sector. The shift to renewable energy sources has the potential to significantly alter the carbon content of power used for battery manufacturing and charging, affecting the ability of PEVs to lower GHG emissions [11]. Many studies assessing the environmental impact of PEVs assume a fixed carbon content of electricity, neglecting the dynamic changes in the generation mix globally. This study incorporates PEV well-to-wheel emissions and anticipated energy mix changes using a condensed life-cycle assessment method. Results emphasize the importance of utilizing the carbon budget promptly, as waiting for cleaner PEV battery production cannot compensate for emissions from combustion vehicle use.

The growing boundaries on the usage of diesel in transportation underscore the need for the usage of renewable electricity sources to electricity automobiles so one can lower emissions of pollutants and GHGs. Even though research on car carbon emissions has broadly speaking targeted diesel and electric-powered cars, hydrogen gasoline is a likely non-fossil fuel opportunity. This look compares the product carbon footprint (PCF) of an electric-powered vehicle versus a hydrogen gas cell car with the use of the LCA approach, emphasizing the tremendous effect of the fuel cycle on PCF. The results underscore the want for extended transparency in sharing PCF method records among car producers for powerful emissions contrast [12].

The transportation industry faces challenges and opportunities amid pollution, climate change concerns, and evolving regulations. With the Paris Agreement and

restrictions on ICEVs, a shift toward EVs is evident. The significant decline in battery prices and enhanced performance contribute to the rapid adoption of EVs. Despite challenges like the shift to shared mobility and autonomous vehicles, the article discusses the main trends and technological challenges in electrifying road transport [13].

A meta-analysis of EV LCAs reveals methodological and data transparency challenges. Environmental breakeven points for each European Economic Area (EEA) nation are calculated based on life-cycle GHG emissions data. The study identifies a subset of EEA nations where EVs may produce more life-cycle GHG emissions than equivalent diesel alternatives. The findings emphasize the need for clearer methodologies and data sharing in EV LCA studies and highlight the policy implications for nations with varying GHG electric grid intensities [14].

A study in Qatar compares the environmental efficiency of electric and conventional petrol cars, considering the carbon footprint associated with non-renewable energy sources. The well-to-wheel life-cycle assessment shows that electric cars perform significantly better than traditional petrol vehicles in terms of emissions. However, the study reveals a lack of motivation among consumers in Qatar to favor electric mobility, suggesting the need for government incentives to achieve the ambitious goal of decarbonizing road transport [15].

Examining the electrification of transport, the study explores various aspects such as environmental benefits, consumer side effects, battery technologies, and socioeconomic benefits. It emphasizes the need for cleaner electricity production methods alongside electrifying transportation. The research indicates a correlation between lower EV ownership costs and greater social fairness, and it discusses challenges related to charging infrastructure and grid management [16].

Then the article looks at critiques of the cutting-edge GHG emissions technique used by the Intergovernmental Panel on Climate Change (IPCC) and proposes an environmentally prolonged input–output (EEIO) evaluation. The EEIO evaluation, primarily based on a patron-based technique, objectives focus on allocating GHG emissions to the very last customers continually. It addresses issues about the applicability of a primarily client-based method and suggests strategies to lessen GHG emissions [17].

Diesel and fuel-powered passenger vehicles contribute considerably to GHG emissions and air pollutants inside the transportation area. The combustion of traditional fuels in cars releases diverse chemical compounds such as solid particles, nitrogen oxides, carbon monoxide, and carbon dioxide into the atmosphere. The study emphasizes the importance of using environmentally pleasant transportation alternatives, particularly in urban areas, to mitigate high concentrations of pollution. Even as EVs provide a cleaner alternative, their environmental effect is inspired by using the power resources used for charging. In international locations such as Poland, heavily reliant on fossil fuels for energy, the oblique emissions from EVs are probably comparable to or maybe higher than direct emissions from traditional cars [18]. The research aims to assess carbon dioxide emissions and environmental impacts associated with regular EV use on a global and national scale, considering different vehicle types (City, Sedan, and SUV).

Worries about the medical consensus on human activities contributing to current climate exchange persist despite rigorous speculation checking out since the 1800s. The article examines previously tried methods to quantify this consensus by way of inspecting a dataset of 88,125 climate-related papers released since 2012. A random subset of 3000 papers and a pattern-weighted method with unique keywords diagnosed by four skeptical papers explicitly or implicitly thinking about human-caused global warming. The evaluation concludes with a high degree of statistical confidence that the clinical consensus on human-caused climate exchange in peer-reviewed literature surpasses 99% [19].

2. Vehicle Performance Criteria

The proposed vehicle specifications are based on several key considerations [20]:

1. ***Speed*:** The vehicle is designed to operate at a maximum speed of 70 mph (112 km/h), adhering to the speed restriction in the UK. The rated motor power, lowest gear ratio, and battery capacity are determined by this maximum design speed.
2. ***Gradeability*:** The vehicle is designed to handle road gradients of up to 20%, allowing it to navigate hills with steeper inclines. The maximum road grade in the UK is 4%, and the vehicle's gear ratio is configured to accommodate the steepest gradients.
3. ***Acceleration*:** The motor's highest torque and gear ratio configuration are decided by acceleration necessities. The automobile makes use of axial air gap everlasting magnet brushed DC vehicles with 50% overload torque capability, making sure perfect acceleration performance in urban areas.
4. ***Driving Range*:** The vehicle is optimized for short trips, with a mean distance of less than 40 km. The battery must maintain a state of charge (SOC) above 20%, even as it approaches the end of its usable life. The vehicle is predicted to travel either at 40 km or 60 km in full electric mode, with the generator activating when necessary to extend the range to at least 300 km.
5. ***Noise*:** The vehicle is designed for brief, low-pace trips, aiming to decrease noise. The electric motor

is quiet, and the combustion engine only turns on, while necessary, with an electricity management device making sure minimum engine operation for noise discount.

6. ***Pollution*:** As a battery-powered EVs, the proposed car produces no local or global pollution when fueled by green energy. The combustion engine only starts when required to achieve the intended journey distance, and an energy management system minimizes engine operation to reduce pollution.
7. ***Vehicle Size*:** A Daewoo Matiz is used as a reference for comparison with real products, ensuring the converted car is comparable in size for accurate assessment.
8. ***Handling/Comfort*:** The vehicle conversion aims to maintain or improve handling and comfort compared to the Daewoo Matiz. Weight distribution improvements contribute to enhanced handling, and the absence of a clutch, reduced motor noise, and vibration improve comfort, especially in urban driving conditions.
9. ***Energy Consumption*:** The target energy consumption for urban driving is 1 to 2 L/100 km of fuel equivalent. The car is designed to run solely on batteries, rechargeable by a wall outlet, with additional consumption at higher speeds due to drag losses, and engine activation for power or range.
10. ***Vehicle Mass*:** Vehicle mass is a critical factor influencing various parameters: lower mass benefits gradeability, acceleration, range, noise levels, and energy consumption. Efforts are made to keep the vehicle mass equal to or lower than the original by designing compact and lightweight battery and motor components.
11. ***Cost*:** The goal is to keep the purchase price comparable to that of a conventional car by maintaining technology simplicity and optimizing battery size. Battery management is implemented to maximize the battery's lifespan and minimize costs.

These specifications reflect a holistic approach to designing a cost-effective, environmentally friendly vehicle suitable for short urban trips.

3. Components Specifications

According to the findings, the adaptive neural fuzzy inference system works well for simulating and regulating automobile engine exhaust emissions.

3.1. Power Requirements

To calculate the necessary power, use the formula below.

$$\text{Rolling resistance}: \Pr(\nu) = Cr \cdot m_{max} \cdot g \cdot \nu \quad (1)$$

where

Cr is the tire rolling coefficient, 0.009
$(m)_{max}$ is the vehicle mass, 680 kg
g is the gravitational acceleration
ν is the vehicle speed

$$\text{Air drag}: P\,air(\nu) = \tfrac{1}{2} \cdot Cd \cdot Af \cdot \zeta \cdot \nu \quad (2)$$

$$\text{Gradient demand}: P\,grad(\text{gradient}, \nu) = m_{max} \cdot g \cdot \nu \cdot \sin(\theta) \quad (3)$$

The following constants have been used

- Gravitational acceleration: g = 9.81 m/s^2
- Air density at 1 bar and 20°C ζ = 1.19 kg/m^3

In equation Pgrad (gradient, ν) each component represents a critical factor in understanding how gradient affects demand during driving.

- **Pgrad**: This is the power required to overcome the gradient.
- **M_{max}**: This is the maximum mass of the vehicle.
- **ν**: This symbol typically denotes the speed of the vehicle.
- **θ**: This is the angle of the gradient, and it directly influences how steep the incline is.

Importance of the gradient angle: The angle θ is crucial as it dictates the level of incline the vehicle has to navigate. A steeper angle leads to a greater component of gravitational force acting against the vehicle's movement, thereby increasing the required power to maintain speed or accelerate. In real-world scenarios:

- **Low Gradient**: A gradient at a lower angle (small θ) results in less required power, making it easier for vehicles to ascend without significant strain.
- **Moderate to Steep Gradient**: As θ increases, the sine value increases, leading to a much larger force opposing the vehicle's movement. For example, a gradient of 30 degrees would require significantly more power compared to a 10-degree slope.

Ultimately, real-world driving is impacted heavily by how vehicles perform under various gradient conditions, affecting fuel consumption, engine load, and overall efficiency.

TABLE 1 The chosen vehicle body attributes.

S/N	Parameter	Value	Unit	Remarks
1	Air drag coefficient (Cd)	0.28	—	Estimated
2	Frontal area (A$)	1.85	m^2	Estimated
3	Tire rolling coefficient (Cr)	0.009	—	Asphalt
4	Mass (m)	680	kg	Shahin
5	Maximum mass (GVW)	1485	kg	Shahin
6	Tire rolling radius (m)	0.286	m	Shahin
7	Engine volume	1.297	cc	Shahin
8	Road gradient	4 (2.3°)	%	Shahin

The total motor power required to move the vehicle up a gradient at speed v is:

$$\text{Power mot}(\text{gradient},v) = \left[\text{Pr}(v) + \text{Pair}(v) + \text{Pgrad}(\text{gradient},v)\right]/\eta\text{mech} \quad (4)$$

The average mechanical drivetrain efficiency is assumed to be 0.9. With its low mass, the chosen vehicle is comparable to a To Shahin. The attributes of the vehicle body are listed in Table 1.

3.2. Propulsion Motor Requirements

The maximum speed and the maximum gradient at this speed decide the power needed by the electric propulsion motor. The details of the switched reluctance motor (SRM) are listed in Table 2. Egypt's high roads have the highest gradient of 4% and 2.3°, with 120 km/h intended top speed. Every calculation is done using the highest mass, m max. The propulsion engine power requirement is Pmot (4 km/h, 120 km/h) 36 kW to reach 120 km/h with a 4% gradient (5). If the speed requirement is relaxed, the motor size might be decreased. Since the maximum speed on Egyptian highways is 100 km/h, the vehicle I designed to travel at that pace while negotiating this 4% gradient will still be in compliance with the rules but allow for a smaller propulsion motor: 26 kW Pmot, cont (4 km/h, 100 km/h) (6).

TABLE 2 Design details of switched reluctance motor (SRM).

S/N	Parameters	Value	Unit
I	**Specifications**		
	DC voltage	650	V
	Peak power	36	kW
	Continuous power	26	kW
	Nominal speed	3000	rpm
	Maximum speed	6000	rpm
II	**Main dimensions**		
	Air gap	0.5	mm
	Rotor lamination ID	144	mm
	Stator lamination OD	281.4	mm
	Lamination stack axial length	117	mm
III	**Windings**		
	Number of phases	3	—
	Number of turns per coil	46	—
	Copper fill factor	0.594	—
	Phase resistance at 20°C	0.41	Ohm

4. Fuel Consumption

According to the technique, the flow rate in liters per 100 km is used to calculate the rationing of fuel consumption. The following formula is used to theoretically assess automobile gasoline consumption Q_z at normal movement (in L (100 km)$^{-1}$) [21] (Tables 7 and 9).

$$Q_z = \text{SEC}\left(P_{rl} + P_w + P_a\right) / 10\rho_f V \eta_T \quad (7)$$

where

Q_z is measured in L/100 km via the following relation: SEC is the optimal specific fuel consumption (kWh kW/h).
P_{rl} is the required power to overcome the rolling road resistance (kW)
P_w is the required power to overcome the air resistance (kW)
P_a is the power required to overcome the inertial acceleration resistance (kW)
ρ_f is the energy density (Wh/L)
V is the automobile movement speed (m/s)
η_T is the energy efficiency

5. Indirect Emission Calculation

5.1. Background

The gasoline consumption and emissions were calculated using a variety of conversions. The calculations needed some assumptions and simplifications due to the tools and techniques used. The volumetric shares of exhaust components are measured by the exhaust gas analyzer used in the research. The shares provide a chance to learn about the quantity of a particular gas released along with data on exhaust gas flow. However, by accounting for the air circulating through the engine's intake manifold and

TABLE 3 The block diagram of promising electric battery types.

Lithium-ion (Lion) The most promising battery technology for electric cars is lithium. Lithium batteries, used in laptops and cell phones, are now offered in big capacities for EV use. Lithium can be produced using a variety of processes. Although lithium polymer batteries generally have the highest energy density, they can catch fire if damaged or overcharged. Lithium iron phosphate batteries are the best choice for use in EVs because they have a slightly lower energy density but are naturally more stable and have a very long cycle life.	
Advanced lead-acid French scientist Gaston Plante invented the lead-acid battery, a type of rechargeable battery, in 1859. It is the first-ever entirely new portable battery architecture. Modern rechargeable batteries are more energy efficient than lead-acid batteries. Despite this, the cells' ability to produce substantial surge currents results in a relatively high power-to-weight ratio.	
Nickel-metal hydride (NiMH) The nickel-cadmium battery, also referred to as the Ni-Cd or NiCad battery, is a type of rechargeable battery that uses nickel oxide hydroxide and metal cadmium as its electrodes. Ni-Cd is an acronym that comes from the chemical symbols for cadmium (Cd) and nickel (Ni). Interestingly, the authorized trademark for NiCad is held by SAFT Corporation, despite the fact that all nickel-cadmium batteries are commonly referred to by this brand name. Wet-cell batteries made of nickel and cadmium were first developed in 1899.	
Nickel-Cadmium Batteries Due to their comparable technological characteristics but superior cycling and energy density, Ni-Cd batteries and lead-acid batteries are in direct competition with one another. A Ni-Cd battery's anode is made of metallic cadmium, while the cathode is composed of nickel oxide hydroxide. Aqueous alkali solution is used as the buffer between the two electrodes in this process. In many portable electronics today, Ni-Cd batteries are used in a similar way to lead-acid and lithium-ion batteries. Despite having superior cycling characteristics and energy density, Ni-Cd batteries have limitations.	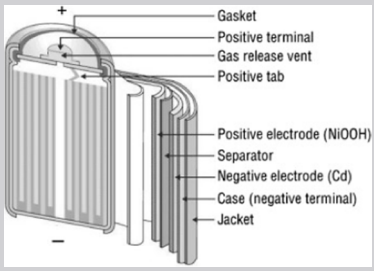
Lead-Acid (PbA) The earliest form of rechargeable battery is lead-acid. Despite being comparatively inexpensive, they are very heavy for their energy and power. The starter engine and 12 V power systems in almost every petrol-powered car are powered by lead-acid batteries. Due to their cheap cost, lead-acid batteries are still commonly used in older EV conversions, but for practical range, a vehicle usually requires batteries that makeup about one-third of its total weight! (Lead sleds are another name for these types of cars.) We favor avoiding lead-acid.	

the fuel dosage, the quantity of exhaust can be calculated. The mass of air and the fuel to be consumed are added to create the mass of exhaust gases. The composition of the exhaust gases can be used to calculate the excess air factor and then to perform the required calculations in place of the direct knowledge of the fuel dose. The Bretschneider's formula and the measured volumetric concentrations of CO, CO_2, HC, O_2, and NOx should be used to calculate the accurate excess air ratio number. For each collection of data gathered during the measurements, calculations were made.

5.2. Indirect Emissions

The emissions that are connected to the extraction, distribution, and transit of the raw materials for the manufacture of fuel are considered indirect emissions. Electricity generation and distribution emissions are considered when deciding whether to use electric or plug-in hybrid cars. Indirect emissions are inversely correlated with the evaluated vehicle's gasoline usage. For light-duty vehicles or two wheelers, the Ecoscore methodology's indirect emission calculation algorithm is as follows:

TABLE 4 EV battery performances.

Battery type	Specific energy (Wh/kg)	Specific power (W/kg)	No. of 80% discharges before replacement	Estimated large-scale production cost (€/kWh)	Anode materials	Cathode materials	Energy density (Wh/L)
Lead-acid (Pb)	35	150	1000	51	PbO_2	Pb	80–90
Advanced lead-acid (Pb)	35–40	180	1500	161	PbO_2	Pb	35–50
Nickel-cadmium (Ni/Cd)	50	200	2000	250	Ni	Cd	50–75
Nickel-metal hydride (NIMH)	70–100	200	2000+	205	Ni	Metal hydride	170–420
Lithium-ion	300	120–150	100+	125	Carbon intercalation	$LiCoO_2$	400

TABLE 5 Indirect emission factors.

Fuel type	CO (mg/kWh)	NMHC (mg/kWh)	NO_x (mg/kWh)	PM (mg/kWh)	CO_2 (mg/kWh)	SO_2 (mg/kWh)	N_2O (mg/kWh)	CH_4 (mg/kWh)
Petrol	18.4	761.4	151.9	8.6	33,100	236.2	0.0	62.0
Diesel	16.6	315.4	129.6	3.6	24,500	174.2	0.0	56.5
CNG (G20)	5.0	99.0	38.2	2.9	14,759	60.8	0.0	805.3
LPG	14.8	202.7	116.3	3.4	21,600	14.1	0.0	58.0
Biodiesel (RME)	493.1	280.4	871.9	66.6	–172,786	245.5	0.0	0.0
Hydrogen	0.033	—	0.082	—	15.4	0.040	—	0.030
Elec. renew	0.0	0.0	0.0	0.0	0.0	0.0	0.0	0.0
Elec. Belg. 03	30	44	392	42	277,683	388	1.558	3.56

$$E_{i,j,indirect} = \frac{1}{3 \cdot 6 \cdot 10^{11}} F_j \cdot \rho \cdot EC \cdot FC \quad \left[kW / km\right] \qquad (8)$$

where

F_j is the factor of indirect emission for pollution J, expressed in mg/kW·h (see Table 5)

ρ is the fuel density expressed in g/L

EC is the energy content of the fuel, expressed in kJ/kg

FC is the fuel consumption of the vehicle, expressed in L/100 km (in the case of light-duty vehicles or two wheelers)

The factor $1/3, 6 \cdot 10^{11}$ in this formula is a conversion factor

Consumption statistics for heavy-duty automobiles are provided in grams per kilowatt-hour, making the aspect in Equation 1 unnecessary. Table 5 incorporates the oblique emission factors (F_j) used in Equation 1. The EU MEET observer's emission factors describe the traditional fuels (petrol, diesel, and LPG) [22]. The fuel consumption for natural gas is measured in cubic meters per 100 km. Because of significant variations in the energy content of natural gas (both poor and rich), the composition of natural gas in Belgium was compared with various fuel data. The G20 was selected for comparison as it is the most similar natural gas. The indirect emissions data for biodiesel gas are primarily based on the MEET regarding alternative emissions and the well-to-wheel analysis of preferred vehicles [23] for CO_2 emissions.

Non-GHG emissions: Although studies on the production of liquid fuels from biomass have addressed the non-GHG effects, only one study [24] was identified that specifically looked at the production of hydrogen from biomass. This source gave data for g/kWhH_2 emissions of VOC, CO, NOx, particulates, and SOx, calculated using GREET. The numbers given are not thought to be reliable for UK policymaking because this one study does not focus on the UK and only examines a small subset of emission types.

6. Standard Driving Cycle Types

6.1. US Driving Cycles

6.1.1. US06 (City Mode Driving Cycle) To address the FTP-75 test cycle's shortcomings in the modeling of aggressive, high-speed and/or quick acceleration driving

TABLE 6 Test matrix to driving cycles information.

Electric vehicle (EV) batteries types	Av. speeds (km/h)	Max. speeds (km/h)	Distance (m)	Duration (s)	Remarks
European test cycles					
ECE 15 (urban driving cycle)					
Lithium-ion	13.7	50	4052	780	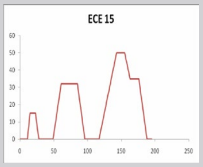
Lead-acid (Pb)					
Nickel-metal hydride (NIMH)					
Nickel-cadmium (Ni/Cd)					
Advanced lead-acid (Pb)					
European test cycles					
EUDC (extra-urban driving cycle)					
Lithium-ion	62.6	120	685	400	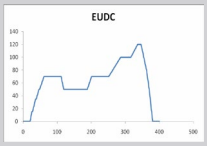
Lead-acid (Pb)					
Nickel-metal hydride (NIMH)					
Nickel-cadmium (Ni/Cd)					
Advanced lead-acid (Pb)					
US driving cycles					
US06 (city mode driving cycle)					
Lithium-ion	78	129	12,892	596	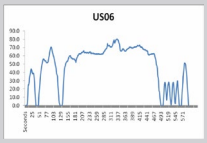
Lead-acid (Pb)					
Nickel-metal hydride (NIMH)					
Nickel-cadmium (Ni/Cd)					
Advanced lead-acid (Pb)					

behavior, rapid speed fluctuations, and driving behavior after starting, the US06 Supplemental Federal Test Procedure (SFTP) was created. The 13 km trip on the SFTP US06 circular takes 10 min, averages 77 km/h, and tops out at 130 km/h. There are four stops in all, and the rapid acceleration has a top speed of 13.62 km/h (or mph) per second. There is no use of the air conditioner, and the engine begins to warm. The temperature of the atmosphere varies from 68°F (20°C) to 86°F (30°C). The cycle's 12.8 km course has a top speed of 80.3 km/h, and it lasts for 6.2 European test cycles. (See Table 6 for details.)

6.2. ECE-15 (Urban Driving Cycle)

According to the data plotted from 0 s to 780 s, which was replicated four times, the extra-urban driving cycle (EUDC) cycle is validated from 780 s to 1180 s. The ECE R15 cycle, also known as the urban driving cycle, was first introduced in 1970 as part of the ECE vehicle regulations. The most recent version is described by ECE R83, R84, and R101. The cycle features a maximum speed of 50 km/h, operates under low engine load, and experiences occasional exhaust gas temperature changes to simulate typical driving conditions in congested European towns. The car begins with a 11 s pause after starting the engine, during which it spends 6 s in neutral (with the clutch engaged) and 5 s in first gear (with the clutch disengaged). It then slowly accelerates to 15 km/h over 4 s, cruises at a constant speed for 8 s, and comes to a complete stop in 5 s (with the last 3 s in neutral and the clutch disengaged). After stopping for 21 s (16 s in neutral, followed by 5 s in the first gear), the vehicle resumes by cruising for 24 s before gradually decelerating to a complete stop in 11 s (the last 3 s with the clutch disengaged). Following another 21 s pause, the car accelerates to 32 km/h over 12 s (5 s in first gear, 2 s to shift gears, and then 5 s in second gear), followed by 16 s in neutral and 5 s in first gear. At 117 s, the vehicle accelerates to 50 km/h in 26 s (5 s in first gear, 9 s in second gear, and 8 s in third gear, and an additional 2 s for gear changes). It then cruises for 12 s, decelerates to 35 km/h for 8 s, continues cruising for another 13 s, and finally brakes to a complete stop in 12 s (2 s to shift to second gear while in neutral with the clutch engaged). After traveling a theoretical distance of 1017 m, the cycle concludes at 195 s and then repeats itself four time. The average speed throughout the cycle is 18. 77 km/h, encompassing a total duration of 780 s (13 min) and covering a theoretical distance of 4067 m. (See Table 6 for additional details.)

6.3. Extra-Urban Driving Cycle

According to the EUDC (greater city driving cycle), which was first established in 1990 by ECE R101, the cycle was

designed to represent aggressive, high-speed driving patterns. The maximum speed of the EUDC cycle is 120 km/h, while low-powered vehicles are only allowed to travel at 90 km/h. After a 20-s stop, if the vehicle has a manual gearbox, it accelerates gradually to 70 km/h over 41 s (manual: 5 s in the first gear, 9 s in the second gear, 8 s in the third gear, and 13 s in the fourth gear, plus an additional 32 s for gear changes). The vehicle then cruises at this speed for 50 s (manual: in fifth gear [sic]), followed by a deceleration to 50 km/h in 8 s (manual: 4 s in the fifth gear). At 201 s, the vehicle travels at 70 km/h for 50 s (manual: in fifth gear), before gradually increasing its speed to 100 km/h in 35 s and maintaining that speed for 30 s (manual: in fifth or sixth gear).

At 316 s, the vehicle ultimately slowly accelerates to 120 km/h in 20 s, cruises for 10 s, and then gradually comes to a complete stop in 34 s (manual: in gear for the last 10 s with the clutch disengaged). It then idles for an additional 20 s (manual: in neutral). The average speed throughout the cycle is 62.6 km/h, with a total duration of 400 s (6 min 40 s), covering an estimated distance of 6956 m. (See Table 6 for additional details.)

7. Modeling of EV

7.1. Description

The suggested system consists of a battery, motor, controller, power converter, and automobile body. The motor is fastened to the vehicle frame's shaft. The motor is powered by batteries, which are used to provide control via an electricity converter. The power converter adjusts the motor's voltage, which alters the speed of the car. Thus, the essential components of electrical cars are the vehicle body, battery, motor, controller, and electricity converter, as seen in Figure 1. The fundamental principle of the electrical engine concept is magnetism.

The engine uses the battery's electricity to create a magnetic pull that pushes the automobile forward and causes extreme torsion right away. To imitate the concept, a throttle perspective and a brake pedal entrance are given through the power supply. In order to provide information to the energy cycle input, the driver controller must monitor the vehicle's proper velocity.

7.2. Modeling Flow

Figure 2 displays the electric vehicle modelling flowchart. The input from the brake and throttle pedals makes up the force cycle delivery. The energy cycle delivery input is received by the longitudinal riding force controller. The riding pressure controller features three input ports, specifically for grade, pace remarks, and reference pace, and three output ports, specifically for acceleration, deceleration, and statistics. The driving force controller's output is sent to an H-bridge via Simulink, which controls the PWM voltage and physiological sign conversion. 5 V is the specified pulse width for activation. The H-bridge runs on internal power. The DC motor is switched by means of the battery. In order to control movement, the battery [25] is connected to the motor via a power converter.

The voltage applied to the motor is adjusted by the power converter. The DC motor is fastened to the vehicle's axle. The components of the car body include beta, NR, NF, pace, hub, and wind. The vehicle's rear wheels are connected to the vehicle's frame's typical rear force. The vehicle's front wheels are attached to the vehicle's frame's usual front pressure. The wheel hubs are connected to the hubs of the vehicle.

As a result, in order to match drive cycle entrance, the pressure controller must be used to monitor the actual speed of the vehicle. It computes the error by comparing the reference speed and real pace. A proportional essential controller is the controller in use. There may be acceleration if the error is really large. Deceleration

FIGURE 1 Block diagram of electric vehicle modeling.

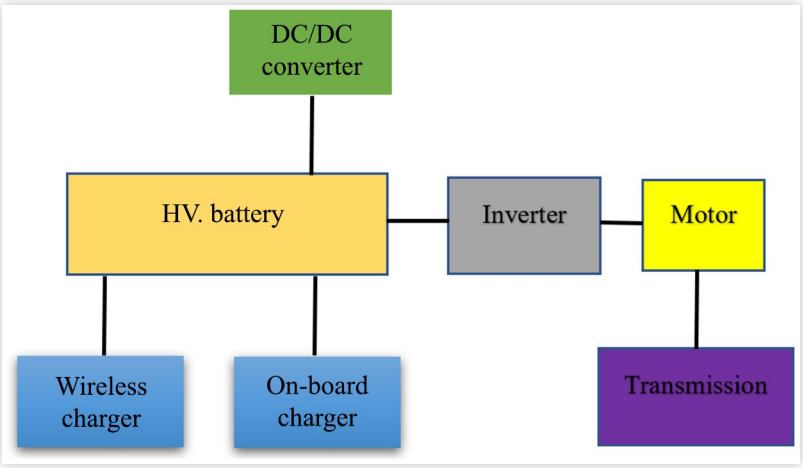

FIGURE 2 Flowchart of electric vehicle modeling.

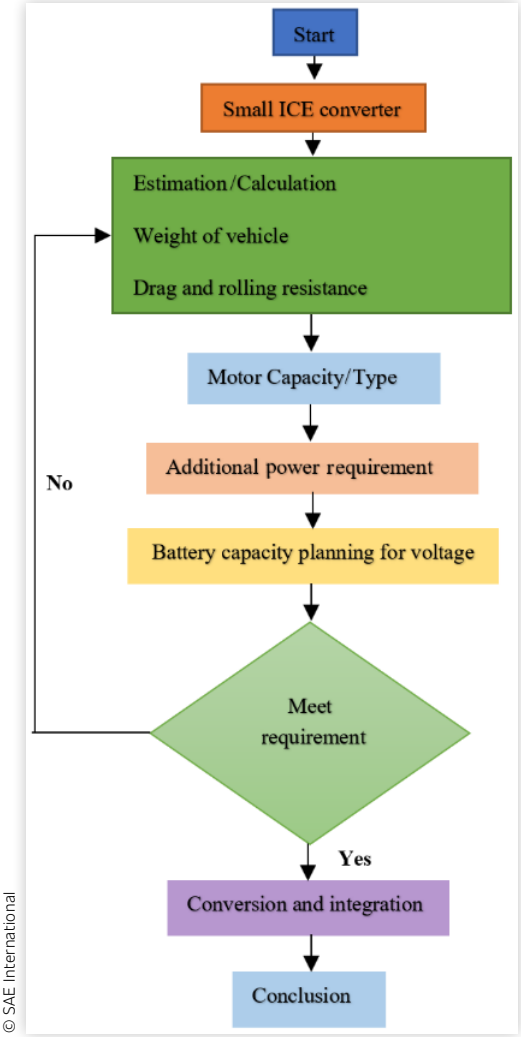

movement may be done inside the vehicle if the mistake is extremely bad.

7.3. Software Description

MATLAB-Simscape is the software used, which enables the rapid building of physical framework models and the use of Simscape within the Simulink environment. Physical issue models help institutions that directly integrate with block diagrams, and distinct model paradigms are developed in the process. Important parts are directly gathered into a schematic by electrical engines, bridge rectifiers, stress-driven actuators, refrigeration frameworks, and other frameworks. Simscape extensions offer more sophisticated functionality and assessment options. Simscape creates deceptive frameworks and assesses how well gadget diplomacy is used.

7.4. Drive Cycle Source

The brake pedal and throttle angle make up the power cycle supply, it is provided as the longitudinal motive force controller's reference input sign.

7.5. Driver Controller

This unit produces normalized acceleration and braking directions by comparing the reference and notes sign (velocities). It serves as a fault detector.

7.6. Power Converter

PWM and Averaged are the two simulation modes available for this block. Its output generates a controlled voltage that is consistent with the input signal at the PWM port.

7.7. Battery

This block offers electricity to strengthen the vehicle accessories in an electric force vehicle.

7.8. Motor

This block uses the electricity from the battery supply to help drive the car's wheels. The DC motor is appropriate for traction applications due to its high starting torque potential. These motors are capable of withstanding an unexpected spike in load without losing control.

7.9. Vehicle Body

This block is a valuable resource for a two-axle car with drag houses, geometry, configurable mass, longitudinal dynamics, and movement. Equal wheel period is a concept. Moreover, its center of gravity is at or below the moving aircraft.

7.10. Ideal Rotational Motion Sensor

One type of mechanical rotational motion sensor is the rotational motion sensor. The measured variable is converted as a control sign in step with the angular speed or attitude between two mechanical rotational hubs.

7.11. Ideal Translational Motion Sensor

Using a translational motion sensor, the measured variable is changed as a manipulable flag between mechanical translational hubs in accordance with the position velocity.

Conventional motors employ fuels generated from petroleum to provide excellent performance and a wide range of speeds. There are a few risks associated with using petrol or diesel, such as low gas mileage and pollutants from exhaust fuel that pollute the environment. This article discusses the creation of an EV mode as a means of overcoming such issues.

8. Research Methodology Flowchart

Using Creately's smooth online diagram editor the diagrams were edited, collaborated with others, and the effects exported to multiple picture codecs. A research method flowchart illustrates the systematic technique used to conduct studies, depicting the sequential steps concerned with collecting data, studying findings, and drawing conclusions. It serves as a visual guide for researchers to navigate the studies technique, ensuring methodological rigor and consistency of their investigations (see Figure 2).

9. Neuro-Fuzzy ANFIS

Imposing a simple Sugeno–Takagi controller within the subject of synthetic intelligence, the designation neuro-fuzzy refers to mixtures of artificial neural networks and fuzzy logic (see Figure 3).

9.1. Overview

Neuro-fuzzy hybridization yields a hybrid intelligent apparatus that combines the learning and connectionist form of neural networks with the human-like reasoning style of fuzzy structures. In the literature, neuro-fuzzy hybridization is frequently referred to as fuzzy neural networks (FNNs) or neuro-fuzzy machines (NFS). The more popular term "neuro-fuzzy tool" refers to a combination of a language version, a challenging and quick set of IF–THEN fuzzy rules, and fuzzy devices that mimic human thinking in fuzzy structures. The main advantage of neuro-fuzzy systems is their conventional approximations and their capacity to request comprehensible IF–THEN rules.

FIGURE 3 Sketch of a neuro-fuzzy system.

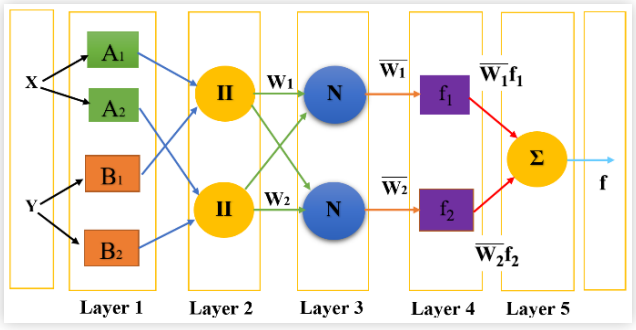

Interpretability, as opposed to accuracy, is one of the two contradicting needs in fuzzy modeling that contribute to the electricity of neuro-fuzzy systems. One of the two households wins the workout. In fuzzy modeling studies, the neuro-fuzzy domain is split into two regions: linguistic fuzzy modeling, which emphasizes interpretability and is mostly focused on the Mamdani model; and specific fuzzy modeling, which is primarily focused on accuracy and is primarily focused on the Takagi–Sugeno–Kang (TSK) model.

Despite the widely held idea that connectionist networks represent a fuzzy system, this period is also utilized to explain a few more configurations in conjunction with:

- Making fuzzy policies with expert RBF networks.
- Neural community training parameters are generally tuned via fuzzy common sense.
- Imprecise norms of sound judgement for creating a community time.
- Fuzzy club feature information obtained through clustering techniques in unsupervised research using SOMs and neural networks.
- Using multi-layer feeds to represent fuzzy inference, defuzzification, and fuzzification in advanced connectionist networks

9.2. Adaptive Neuro-Fuzzy Inference System

The result is the sum of the products of the effects and the weights of every rule. In phrases of capability, an ANFIS and a Takagi-general practitioner (T-S) fuzzy inference machine are equal. The ANFIS set of rules adjusts the club capabilities and different parameters based totally on the input–output training statistics pairs, the use of returned propagation gradient descent, and least rectangular kind methods.

Those methods make the ANFIS modeling more methodical and less reliant on specialized expertise, growing its objectivity. More records regarding the correspondingly comparable ANFIS structure and schooling procedure can be observed in [26, 27].

10. ANFIS Model Design

10.1. Input Identification

Earlier than schooling the individual ANFIS model, it's far crucial to decide the appropriate quantity of enter club functions inside the preliminary condition.

Before educating every ANFIS model, the wide variety of enter club capabilities is decided, which is a full-size part of the initial state. The ANFIS instance has N inputs, okay club features for every enter, and R fuzzy rules.

$$R = K^N \tag{9}$$

The regulations of inference and, as a result, the education time and reminiscence usage of the ANFIS version may be notably extended by way of a large number of inputs and enter membership functions, based totally on Equation 9. As a result, an enter choice should be achieved that assesses the significance of every filter out enter and makes a nice use of it. Fuzzy neural modeling input selection may be performed quickly and without problems with ANFIS. The idea in the back of the advised enter selection method is that an ANFIS model with a decreased RMSE (square root common blunders) after one training duration will have a better likelihood of doing so while given extra education durations. Five models had been studied and trained to use the micro-rectangular method using exclusive combos of two entries [28, 29].

10.2. Training Process for ANFIS Model

The NF community, that's linked to the automobile in series, is the primary element of the ANFIS paradigm. Figure 4 indicates the education procedure for growing the vehicle version, wherein enter and output facts units are used to mirror the enter-output homes of car emissions. The training data set is based totally on the subsequent variables: CO, CO_2, NOx, HC, PM, and MNOx, in which CO denotes carbon monoxide, CO_2 denotes carbon dioxide, NO_X denotes nitrogen oxides, and HC denotes unburned hydrocarbons. The desired car engine emission is MNO_{xd}. The nitrogen oxides are what make up NO_x, which allows you to decrease the cost characteristic errors, E, as given by Equation 10.

$$E = \sum\left(NO_x - MNO_{xd}\right) \tag{10}$$

FIGURE 4 ANFIS model for the vehicle inputs.

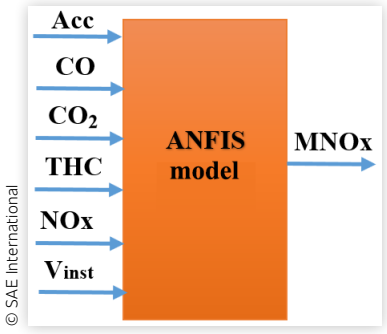

The least square estimate approach may be used to educate the ANFIS network, with MNO_{xd} serving because the matching real (desired) output of the issue's ANFIS and NO_X serving as the input sign. By using repeatedly acting the necessary paintings over a set quantity of time, the iterative studying tuner seeks to beautify the tracking performance of inverse-ANFIS manipulation.

10.3. ANFIS Model Performance Criteria

The kind and quantity of club activities substantially have an effect on ANFIS's overall performance. After evaluating a number of club features, it's far determined that ANFIS, which makes use of the Gaussian curve membership feature (gaussmf), performs better at forecasting automobile engine emissions underneath distinct combinations of the two parameters. Furthermore, ANFIS showed improved performance up to an education period count number of 200, but now not past that factor. Accordingly, 200 was determined to be the finest variety for the training session. The accuracy of the ANFIS in predicting car engine traits changed into evaluated by measuring the correlation coefficient (R) and root imply square error (RMSE) of the ANFIS model after the optimum values have been chosen. The TSK fuzzy rule, a kind-three fuzzy rule with a linear mixture of inputs and as regular as the consequent portion, is simulated via the ANFIS software. The very last output of the machine is weighted by the common effects from each rule. To decide how effectively a technique predicts, two standards are established. The look at standards where the correlation coefficient (R) and the root imply rectangular blunders (RMSE). The correlation coefficient (R) indicates how closely the experimental and anticipated findings suit each other.

$$R(a,p) = \frac{\operatorname{cov}(a,p)}{\sqrt{\operatorname{cov}(a,a)\operatorname{cov}(p,p)}} \tag{11}$$

where cov (a, p) is covariance between a and p sets, a and p denote the actual output and predicted output sets, RMSE is determined by

$$RMSE = \sqrt[4]{\frac{1}{n}\sum_{i=1}^{n}\left(a_i - p_i\right)^2} \tag{12}$$

The ANFIS model's performance in training and testing sets is verified using statistical measures such as R(a, p), RMSE, and others, which are commonly employed in iterative prediction and optimization systems. On the other hand, an affiliated adaptive neuro-fuzzy inference machine (ANFIS) version has been formulated for predicting the output parameters,

namely brake thermal efficiency (BTE), brake specific energy consumption (BSEC), oxides of nitrogen (NOx), unburned hydrocarbon (UBHC), and carbon monoxide (CO) via thinking about the engine load and butanol proportion inside the blend as input parameters. As the percentage of butanol in the diesel–butanol blend increases, both the BTE and BSEC significantly improve, while exhaust gas emissions, especially NOx and CO, are reduced. An advanced AI model based on ANFIS is capable of accurately mapping the relationship between input and output parameters of the CRDI engine. In this study, the statistical performance metrics derived from ANFIS model are (0.0000107–0.0000755) for mean square error, (0.000353–0.001533) for mean square relative errors, (0.999722–0.999939) for the correlation coefficient, and (0.999444–0.999878) for the absolute fraction of variance. These results enhance the model's capabilities to a higher level under diesel–butanol conditions.

10.4. Development of ANFIS Model Simulink

The Simulink version of the complicated parameters of the car became constructed using MATLAB R2015a. The toolboxes for the electricity machine, energy electronics, manipulate machine, sign processing, and essential functions have been among those used to construct this Simulink model. The Simulink model consists of a number of different additives, consisting of clocks, subsystems, integrators, output sinks (scopes), input assets, workspace blocks, constants, buses, mux, de-mux, summers, adders, advantage blocks, multipliers, consistent blocks, CT & DT blocks, ANFIS editor blocks, and much more. The developed Simulink model for regulating several automotive emission parameters is shown in Figure 5.

FIGURE 5 Simulink of neuro-fuzzy model.

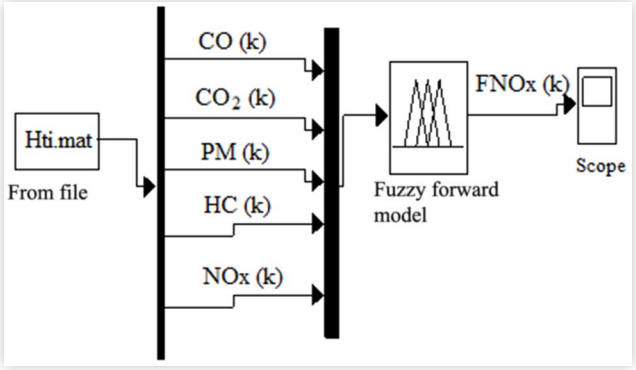

11. ANFIS Controller Design

11.1. Background

At some point in the layout phase, the ANFIS controller's enter variables for CO, CO_2, NOx, HC, and PM all got here into being. However, a chassis dynamometer that takes a look at cells is normally the handiest location to locate CO, CO_2, NOx, HC, and PM trying out gadgets. They're not journeying in any Fiat Petra cars. As a result, even as this ANFIS controller is beneficial for figuring out the great approaches to control CO, CO_2, NOx, HC, and PM in a chassis dynamometer test cellular, it cannot be applied to control these pollutants in an automobile on the street while emission analyzers are not to be had. This problem becomes addressed by way of suggesting the ANFIS controller [30].

11.2. Procedure for ANFIS Controller Training

The usage of input/output data sets allows ANFIS to construct a fuzzy inference system (FIS) and adjust the membership function parameters through a backpropagation algorithm. To ensure effective tuning of the membership functions, all possible data variations must be covered, requiring a sufficiently large dataset. The dataset includes variables such as CO, CO_2, NOx, HC, PM, and CNOx (Figure 6). The ANFIS controller is implemented using MATLAB, based on experimental datasets. A total of 3048 statistics samples were collected for a vehicle with a target speed of 50 km/h and a maximum speed of 80 km/h. While the vehicle is traveling at 50 km/h, the instantaneous speed (Vinst) is approximately 60 km/h. The data were split equally into 1524 training points and 1524 verification points. Any number that cannot be evenly divided is referred to as an atypical variety

FIGURE 6 ANFIS controller for the output.

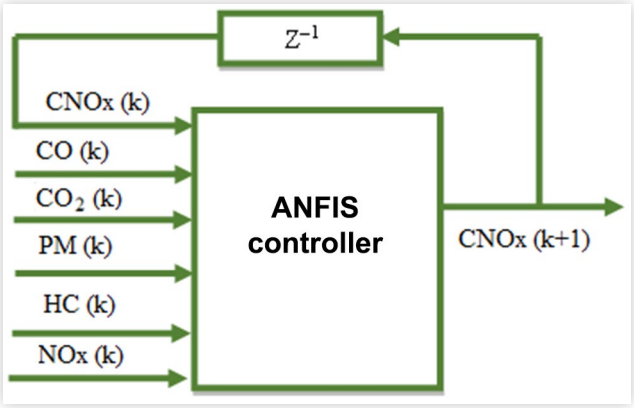

The overall performance of the ANFIS controller is influenced by the education process. The training can be assessed using an error metric that highlights the variations between the ANFIS output and the actual output from the dataset. The fewer errors the model produces after training, the more accurately it has learned. The outputs for managing CO, CO_2, NOx, HC, and PM should be forecasted as accurately as possible. Sub-clustering was employed to develop the FIS, and a hybrid optimization method that combines least-squares and backpropagation gradient descent was utilized to train the FIS controllers. The parameters of the sub-clustering's parameters were cautiously adjusted to decrease errors for the CO, CO_2, NOx HC, and PM controllers.

11.3. ANFIS Controller Performance Parameters

After adjusting variables such as CO, CO_2, NOx, HC, and PM, the usage of the ANFIS controller within the chassis dynamometer's simulation may produce several datasets (matrices). For each dataset, the final column represents the controller's output variable (which could be CO, CO_2, or NOx levels), while each preceding column represents an enter variable (vector), including factors such as vehicle speed or longitudinal acceleration.

The ANFIS controller responds with an output control variable based on the values of the input variables it receives. The ANFIS controllers can determine the relationship between these input variables and the output variable. The processes are modeled through ANFIS.

To train the ANFIS, the final input variables—CO, CO_2, NOx, HC, and PM—can be excluded from the list of input variables. Following training, the ANFIS tool will need require CO, CO_2, NOx, PM, or HC as input variables; instead, it will be able to control CO, CO_2, NOx, and THC in a moving vehicle. Initially, datasets will be created: one for the CO ANFIS controller, another for the CO_2 ANFIS controller, a third for the NOx ANFIS controller, and a fourth for the THC ANFIS controller.

For the CO training set, the input variables are vehicle speed and longitudinal acceleration, with the output being CO. The result for the CO_2 training dataset is CO_2. For the NOx training dataset, vehicle speed and longitudinal acceleration are the input factors, with the output being CNOx. Similarly, the HC training dataset uses the same input variables (vehicle speed and longitudinal acceleration) and the output is CHC.

To incorporate diverse driving into the training datasets, the development model's ECU was provided with a complex load signal curve to collect information on various driving pattern dynamics for the ANFIS.

While a new load signal curve is communicated to the vehicle's electronic control unit, the ANFIS control unit's ability to function independently of driving conditions can be demonstrated. Simulink and MATLAB software are used to develop the ANFIS controller, which is designed in Figure 6 to alter the exhaust emission components of a vehicle's engine.

11.4. Creation of Simulink ANFIS Controller

The Simulink's library toolboxes for energy gadgets, energy electronics, control systems, and sign processing were utilized to develop the Simulink model for the ANFIS console. Simulink played a crucial role in enhancing the overall system, which consists of a reverse ANFIS control unit and a forward NF model, functioning as a closed-loop feedback control system. Figure 7 indicates the Simulink model that was created to modify the NF controller's original parameters.

11.5. Building the Controller

To replicate optimal selections, a controller aims to be enhanced by utilizing a database that contains ideal control choices, inputs, and outputs. This method consistently produces top-rated control outputs, often surpassing the controller itself or relying on a dataset that encompasses all viable values, which can be referenced as needed. However, real-time systems, especially within the transaxle unit of an automobile where quick decision-making is critical, cannot employ such a method. The ANFIS offers a practical solution, where information is gathered though a set of rules, learning occurs offline, and optimal performance is subsequently achieved. By harnessing the generalization and pattern recognition capabilities of artificial neural networks (ANN), a brand-new fuzzy logic system (FLS) is developed to imitate the optimum overall performance. In this study, the MATLAB ANFIS toolbox was used to construct the controller.

11.6. Controller Integration into the Vehicle

The brand-new FLS is derived using the learned parameters obtained during the automatic training of the ANFIS device. The controller can now be integrated into the

FIGURE 7 Simulink of ANFIS controller output.

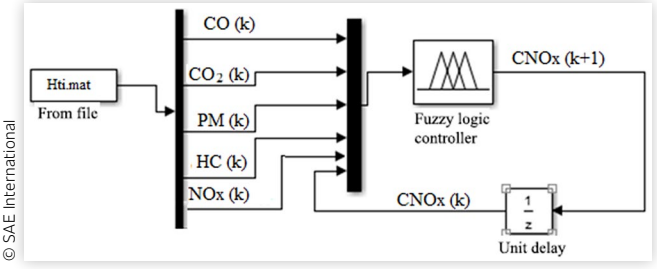

automobile and is imported as a Simulink block, which is then fastened to the automobile. Additionally, an observer gathers data from chassis dynamometer testing and feeds this information into the proposed controller for monitoring exhaust emissions. The automobile is ready for testing under various scenarios after the modules are mounted. On the other hand, actual international emissions and electricity consumption behavior from automobiles are a key element for meeting air quality and greenhouse gasoline (GHG) targets for any country. At the same time, as CO_2 fleet objectives for vehicles are established based on standardized testing procedures, real-world driving situations introduce significant variabilities. Predominant variations contributing to these variations include the driving cycle, vehicle load, driving resistances, ambient temperature levels, starting conditions, ride duration, driver gear-shifting behavior, auxiliary power demands, and fuel quality.

11.7. ANFIS Control Technique Works

Automobiles utilize a car exhaust emission controller to limit the release of toxic gases from engine components, including crankcase, carburetor, and different parts of the engine. These emissions encompass total hydrocarbons (THC), NOx, CO_2, and CO. This guide provides an in-depth look at identifying the characteristics of the tested automobile exhaust and how different components have been designed for exhaust modification. To evaluate the effectiveness of the ANFIS controller, the following relationship is employed: it replaces the RMS of the exhaust emission components controller with the RMS of both the actual output and the output data generated by the ANFIS controller:

$$\text{Effectiveness},\% = \frac{\text{RMS}_{\text{actual}} - \text{RMS}_{\text{controlled}}}{\text{RMS}_{\text{actual}}} \times 100 \quad (13)$$

where

Effectiveness is the ANFIS controller effectiveness (%)
$\text{RMS}_{\text{actual}}$ is the root mean square for actual output
$\text{RMS}_{\text{controlled}}$ is the root mean square for ANFIS controller output

This relationship serves as a quantitative measure to gauge how well the ANFIS controller performs in comparison to the actual emissions, offering insights into its efficacy in managing and reducing harmful gases emitted by the vehicle.

12. Results and Discussion

12.1. EV Powertrain Performance

For EVs, where consumption data is provided in grams per kilowatt-hour, the inclusion of the factor ρ in Equation 7 is unnecessary. The indirect emission factors (F_j) utilized in Equation 8 are available in Table 5. Figures 8–19 display the instantaneous speeds, average total road resistance, power, average specific energy consumption, and average fuel consumptions, which are tabulated in Table 7. These values are based on three driving cycles: ECE 15 (urban driving cycle), EUDC, and US06 (city mode driving cycle).

FIGURE 8 Vehicle speed (ECE-15).

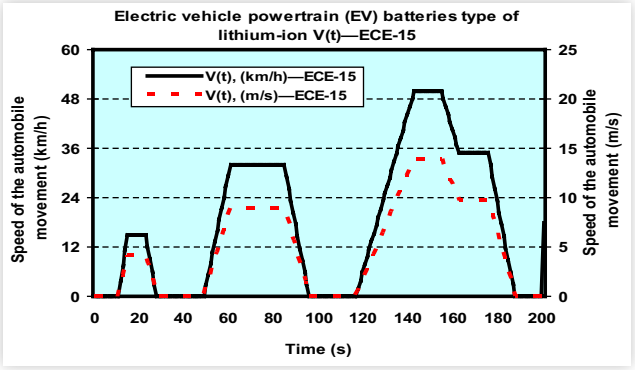

12.2. EV Indirect Emissions Estimation

For EVs, where emission data is presented in parts per million (ppm), the inclusion of the factor ρ in Equation 2 is unnecessary. The indirect emission factors (F_j) utilized in Equation 8 can be referenced from Table 5. Figures 20–24 illustrate the values of emission components, including indirect nitrogen oxide (NOx), indirect carbon monoxide (CO), indirect hydrocarbon (HC), indirect carbon dioxide (CO_2), and particulate matter (PM). These values are based on three driving cycles: ECE 15 (urban driving cycle), EUDC, and US06 (city mode driving cycle), respectively, see Table 8.

FIGURE 9 Vehicle speed (EUDC).

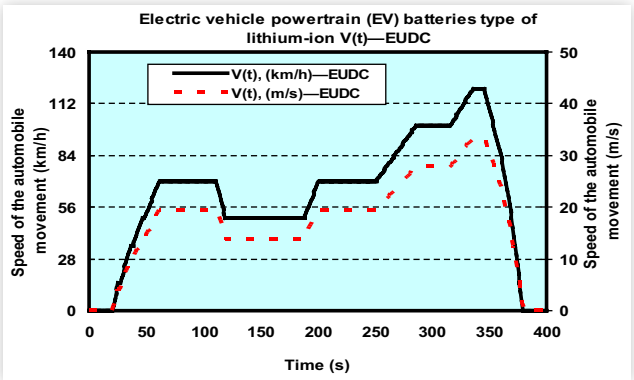

FIGURE 10 Vehicle specific energy (US06).

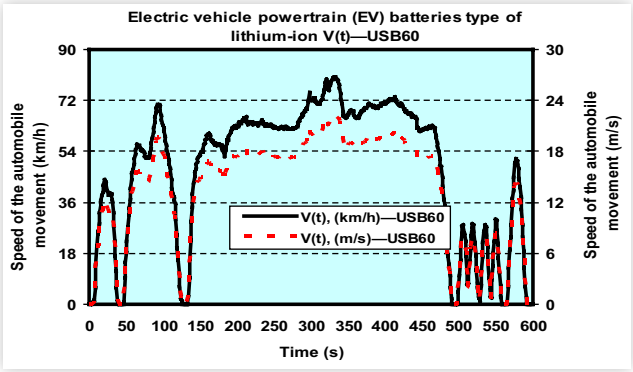

FIGURE 11 Vehicle total road resistance power (P) (ECE-15).

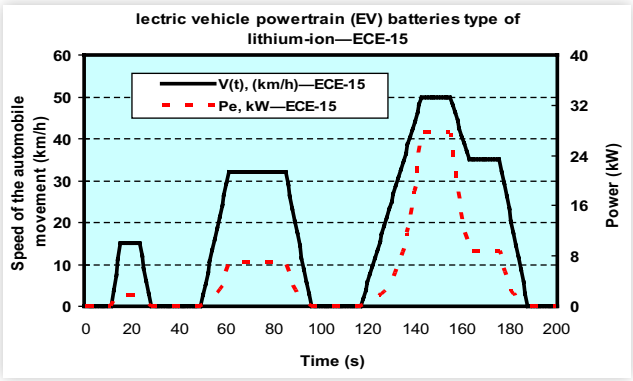

FIGURE 12 Vehicle total road resistance power (P) (EUDC).

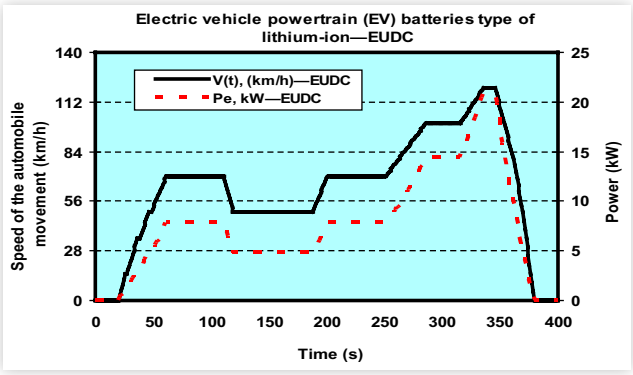

FIGURE 13 Vehicle total road resistance power (P) (US06).

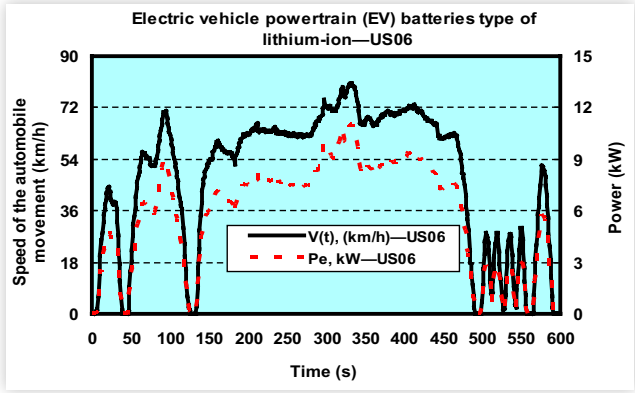

FIGURE 14 Vehicle specific energy consumption (SEC) (ECE-15).

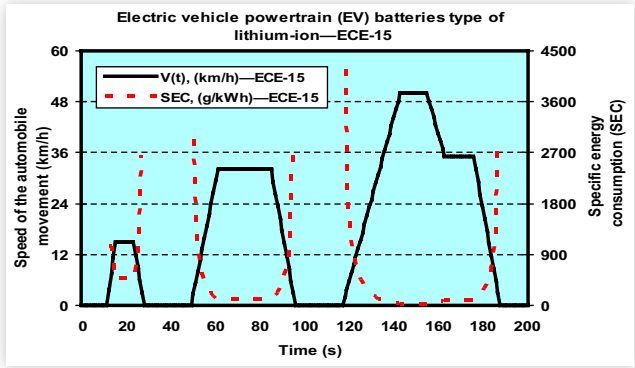

FIGURE 15 Vehicle specific energy consumption (SEC) (EUDC).

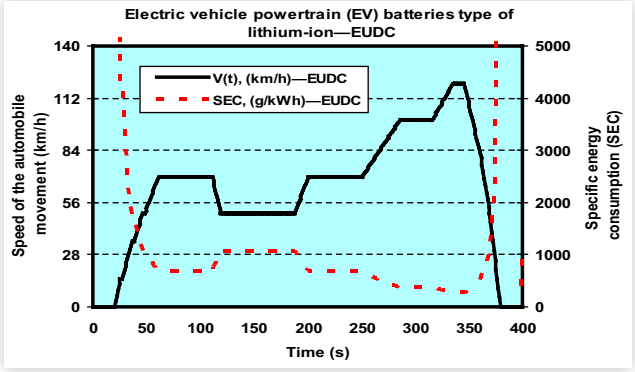

FIGURE 16 Vehicle specific energy consumption (SEC) (US06).

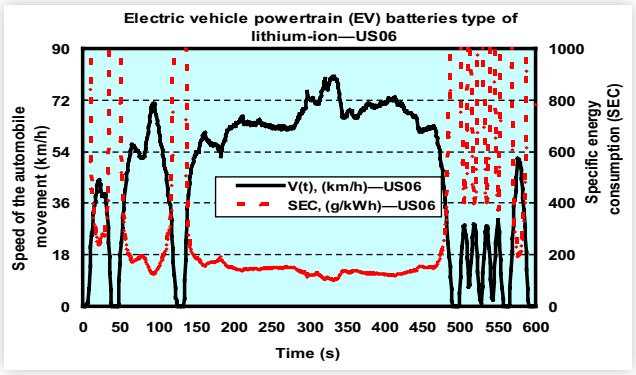

FIGURE 18 Vehicle fuel consumption L/(100 km) (Qni) (EUDC).

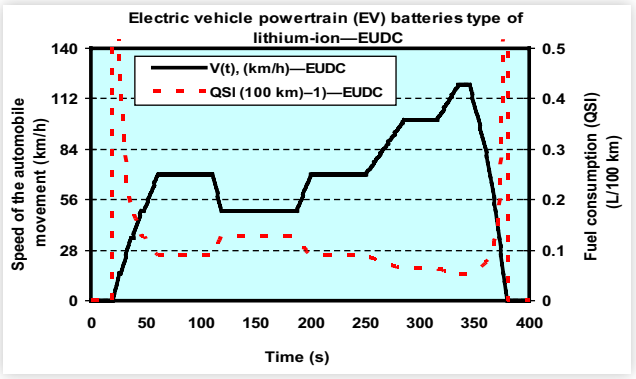

12.3. The Relationship between the Emission Components and Specific Energy Consumption

Based on the information found in Tables 7 and 8, which present the relationship between various emission components and specific energy consumption, tabulated in Table 9, we can take PM exposure as an example. Numerous studies have linked PM exposure to harmful health outcomes, prompting governments to push for a transition to electric passenger automobiles to mitigate air pollution. However, the assessment indicates that electric vehicles may not significantly reduce PM levels as anticipated, largely due to their relatively high energy consumption. By reviewing existing literature on non-exhaust emissions across different driving cycles, it becomes apparent that there is a notable correlation between energy consumption and non-exhaust PM emissions. This correlation is expected to grow as exhaust regulations become stricter and average vehicle energy consumption rises. Consequently, future policies should prioritize setting standards for non-exhaust emissions and promote energy consumption reductions across all vehicles to achieve a meaningful decrease in PM emissions from traffic.

12.4. ANFIS Model Criteria Evaluation

In this study, the ANFIS model structure comprises four hidden layers: the input membership feature, rule base, membership feature, and aggregated output layers. The model has six input neurons and one output neuron. To affirm the accuracy of the model, a dataset of 16,384 data points from measured records were used. The anticipated (model) values were compared with experimental values for car exhaust emissions components (CO, CO_2, NOx, and THC). The model was initially developed using one dataset and was then tested on a second dataset, serving as both input and output. To evaluate its efficacy, Equations 4 and 5 were employed to gauge performance on extra datasets. The correlation coefficient (R) and RMSE for ECE 15 (urban driving cycle) are 0.99 ppm and 103.32 ppm,

FIGURE 17 Vehicle SEC fuel consumption L/(100 km) (Qni) (ECE-15).

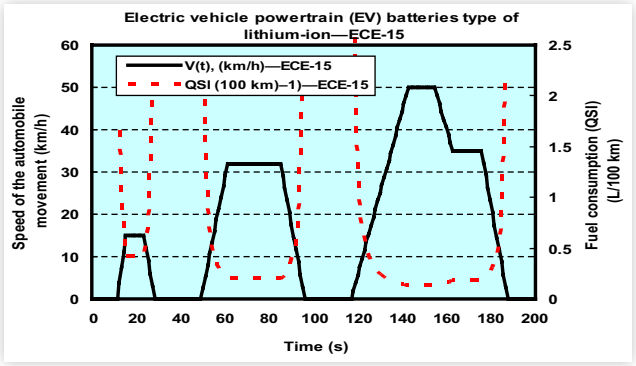

FIGURE 19 Vehicle fuel consumption L/(100 km) (Qni) (US06).

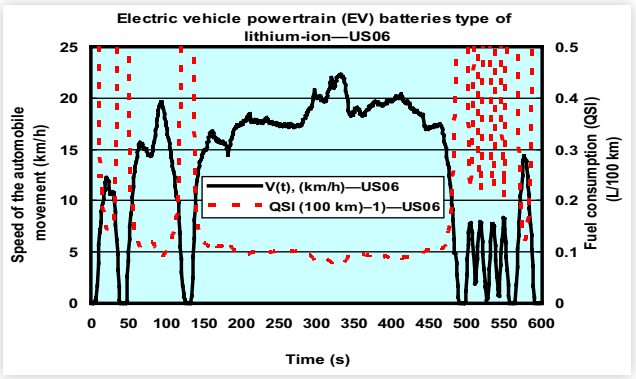

TABLE 7 Predicted real-time performance results for electric vehicle powertrain with different electric batteries.

Electric vehicle (EV) battery types	Speed V(t) (km/h)	Speed V(t) (m/s)	Av. total road resistance power (P) (kW)	Av. specific energy consumption (SEC) (Wh/kWh)	Av. fuel consumption L/ (100 km) (Qni)
European test cycles					
ECE 15 (urban driving cycle)					
Lithium-ion	17.8054726	4.9459646	5.753768	2124.129	0.2672360
Lead-acid (Pb)	17.8054726	4.9459646	5.753768	477.957728	0.2672360
Nickel-metal hydride (NIMH)	17.8054726	4.9459646	5.753768	23330.0152	0.2672360
Nickel-cadmium (Ni/Cd)	17.8054726	4.9459646	5.753768	398.274183	0.2672360
Advanced lead-acid (Pb)	17.8054726	4.9459646	5.753768	284.129358	0.2672360
European test cycles					
EUDC (extra-urban driving cycle)					
Lithium-ion	62.4506234	17.34739	7.660369	874.053351	0.2672360
Lead-acid (Pb)	62.4506234	17.34739	7.660369	477.957728	0.2672360
Nickel-metal hydride (NIMH)	62.4506234	17.34739	7.660369	917.756016	0.2672360
Nickel-cadmium (Ni/Cd)	62.4506234	17.34739	7.660369	724.887273	0.3990029
Advanced lead-acid (Pb)	62.4506234	17.34739	7.660369	4057.74351	0.2672360
US driving cycles					
US06 (city mode driving cycle)					
Lithium-ion	47.9639933	13.32333	5.753768	2124.129	0.0387569
Lead-acid (Pb)	47.9639933	13.32333	5.753768	521.4241	0.0277420
Nickel-metal hydride (NIMH)	47.9639933	13.32333	5.753768	2354.172	0.0269453
Nickel-cadmium (Ni/Cd)	47.9639933	13.32333	5.753768	434.5201	0.0278511
Advanced lead-acid (Pb)	47.9639933	13.32333	5.753768	292.3126	0.0278577

FIGURE 20 Carbon monoxide (CO).

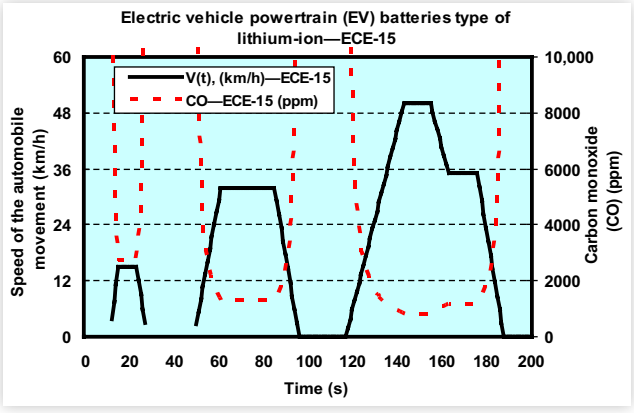

FIGURE 21 Nitrogen oxide (NOx).

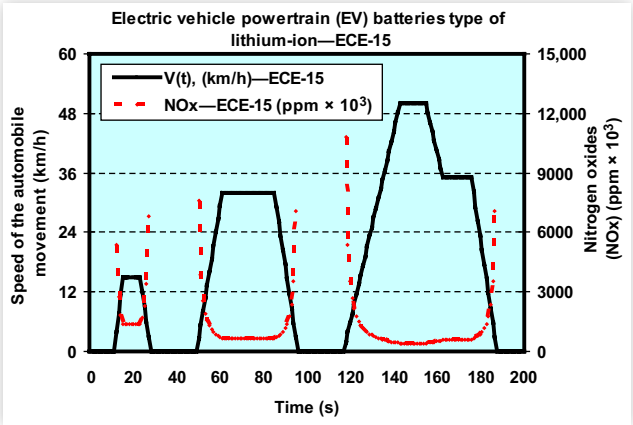

FIGURE 22 Carbon dioxide (CO_2).

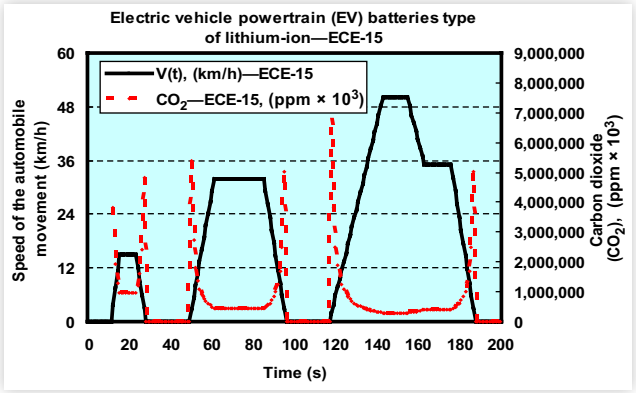

FIGURE 24 Particulate matter (PM).

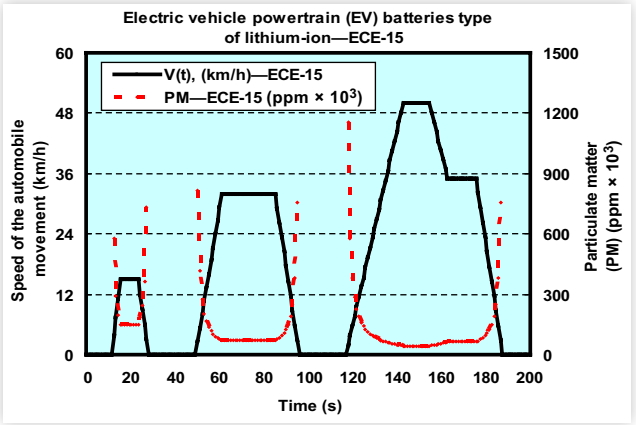

respectively. For EUDC, R is 0.69 with an RMSE of 83.63 ppm, and for US06 (city mode driving cycle), R is 0.24 with an RMSE of 2778.5 ppm. The predictions for carbon dioxide (CO_2) yielded an R of 0.02 and an RMSE of 2907.7 ppm. For the EUDC, R is 0.170 with an RMSE of 60.06 ppm, while for the sequential gas injection, R is 0.47 with an RMSE of 1954.3 ppm. ANFIS predictions for NO_X resulted in R values of 0.57 for the ECE 15 (urban driving cycle), 0.793 EUDC, and 0.91 (US06 (city mode driving cycle)), accompanied by their respective corresponding RMSE values. ANFIS forecasts for unburned hydrocarbons (THC) showed R and RMSE values for continuous gas injection of 0.26 and 2860.9 ppm, respectively. For EUDC , R is 0.310 with an RMSE of 3559.2 ppm, and for US06 (city mode driving cycle), R is 0.67 with an RMSE of 2720.0 ppm, see Table 10. These outcomes demonstrate ANFIS's ability to accurately predict exhaust emission parameters, with errors generally within acceptable thresholds. However, some data values exceed these thresholds and are considered outliers, primarily due to their occurrence during brief load periods. To identify the best and most relevant rules, the following section will explore the training of a neural network using a fuzzy rule base, employing an ANFIS controller.

FIGURE 23 Hydrocarbon (HC).

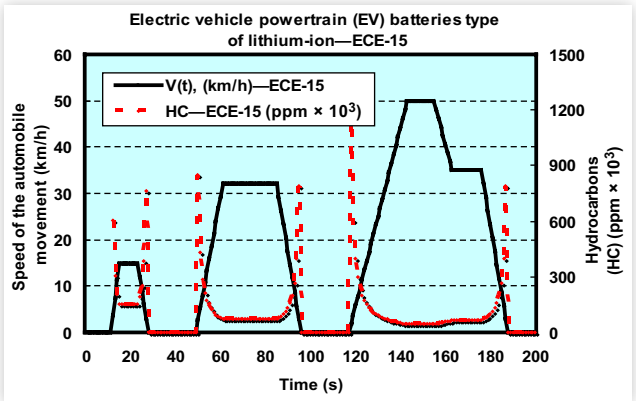

12.5. Provide Possible Applications of Your Results

Car engines (both gasoline and diesel) have the potential to run on alternative fuels, such as homogeneous charge compression ignition (HCCI), which are considered some of the most promising energy sources for the future. These fuels offer significant potential for reducing automobile engine exhaust emissions, including both fuel emissions and noise. Consequently, there's an ever increasing global interest in finding ways to minimize the greenhouse effect and other environmental pollutants. It's believed that vehicles powered by alternative fuels can dramatically reduce dependence on fossil fuels while significantly lowering tailpipe emissions and noise pollution. Using fuels such as CNG, hydrogen, alcohol, methanol, or biofuels can open up new pathways for energy storage and distribution from abundant, locally available sources while also reducing carbon footprints. It is expected that the use of alternative fuels will gain a strong foothold in the automotive industry, potentially achieving three times the energy efficiency of internal combustion engine vehicles with comparable performance, all while emitting no air pollutants. Historically, there has been a transition from solid to liquid to gaseous fuels as primary energy sources. In the coming decades, road transportation is likely to continue contributing significantly to urban air pollution. Many trips within cities are substantially shorter than 6 km, and in urban areas, the average emissions per distance traveled are relatively high since catalytic converters are often ineffective during the first few minutes of engine operation. Additionally, a significant portion of pollution emissions stems from poorly maintained vehicles that lack effective exhaust emissions treatment systems.

TABLE 8 The estimation of indirect real-time emissions results for electric vehicle with different electric batteries.

Electric vehicle (EV) battery types	Carbon monoxide (CO) (ppm)	Nitrogen oxide (NOx) (ppm)	Hydrocarbon (HC) (ppm)	Carbon monoxide (CO_2) (ppm)	Particulate matter (PM) (ppm)
European test cycles					
ECE 15 (urban driving cycle)					
Lithium-ion	66,657.1862	871,763.72	97,851.03	617,535,624	93,403.255
Lead-acid (Pb)	1751.31104	1751.311	2568.59	16,210,310.1	2451.8354
Nickel-metal hydride (NIMH)	23,446.6652	305,117.3	34,247.86	217,218,156	31,685.570
Nickel-cadmium (Ni/Cd)	2084.89409	27,242.616	3057.845	19,297,988.2	2918.8517
Advanced lead-acid (Pb)	1111.94351	14,529.395	1630.85	10,292,260.4	1564.5045
European test cycles					
EUDC (extra-urban driving cycle)					
Lithium-ion	26,381.6445	154,953.1	13,190.82	244,191,140	969.52543
Lead-acid (Pb)	694.290788	1880.907	1015.754	6,410,398.97	969.58314
Nickel-metal hydride (NIMH)	115,770.790	455,562.3	115,770.8	85,466,898.7	12,927.005
Nickel-cadmium (Ni/Cd)	989.370557	40,675.21	1443.875	9,157,712.81	1163.4997
Advanced lead-acid (Pb)	25,600.5561	1,301,085	625.7914	3,949,355.13	940.82043
US driving cycles					
US06 (city mode driving cycle)					
Lithium-ion	10,978.76	16,590.1	51,134.55	930,190,648	3129.4152
Lead-acid (Pb)	2615.006	2188.73	3835.342	24,204,758.8	3661.0086
Nickel-metal hydride (NIMH)	3660.768	40,675.2	4565.585	28,813,302.5	3660.7690
Nickel-cadmium (Ni/Cd)	99,612.76	455,562.3	51,134.55	15,367,094.8	3660.7690
Advanced lead-acid (Pb)	3659.30334	1,301,085	2434.004	15,360,942.3	340,205.06

TABLE 9 The estimation of indirect real-world emissions results for electric vehicle with different electric batteries.

Electric vehicle (EV) battery types	Carbon monoxide (CO) (ppm)	Nitrogen oxide (NOx) (ppm)	Hydrocarbon (HC) (ppm)	Carbon monoxide (CO_2) (ppm)	Particulate matter (PM) (ppm)	Av specific energy consumption (Wh/kWh)	Av. fuel consumption/ (100 km)
ECE 15 (urban driving cycle)							
Lithium-ion	66,657.18	871,763.7	97,851.03	617,535,624	93,403.255	2124.129	0.2672360
Lead-acid (Pb)	1751.311	1751.311	2568.59	16,210,310	2451.8354	477.95772	0.2672360
Nickel-metal hydride (NIMH)	23,446.66	305,117.3	34,247.86	217,218,156	31,685.570	23,330.015	0.2672360
Nickel-cadmium (Ni/Cd)	2084.894	27,242.61	3057.845	19,297,988	2918.8517	398.27418	0.2672360
Advanced lead-acid (Pb)	1111.943	14,529.395	1630.85	10,292,260	1564.5045	284.12935	0.2672360
EUDC (extra urban driving cycle)							
Lithium-ion	26,381.64	154,953.1	13,190.82	244,191,140	969.52543	874.05335	0.2672360
Lead-acid (Pb)	694.2907	1880.907	1015.754	6,410,398.9	969.58314	477.95772	0.2672360
Nickel-metal hydride (NIMH)	115,770.7	455,562.3	115,770.8	85,466,898	12,927.005	917.75601	0.2672360
Nickel-cadmium (Ni/Cd)	989.3705	40,675.21	1443.875	9,157,712.8	1163.4997	724.88727	0.3990029
Advanced lead-acid (Pb)	25,600.55	1,301,085	625.7914	3,949,355.1	940.82043	4057.7435	0.2672360
US06 (city mode driving cycle)							
Lithium-ion	10,978.76	16,590.1	51,134.55	930,190,648	3129.4152	2124.129	0.0387569
Lead-acid (Pb)	2615.006	2188.73	3835.342	24,204,758	3661.0086	521.4241	0.0277420
Nickel-metal hydride (NIMH)	3660.768	40,675.2	4565.585	28,813,302	3660.7690	2354.172	0.0269453
Nickel-cadmium (Ni/Cd)	99,612.76	455,562.3	51,134.55	15,367,094	3660.7690	434.5201	0.0278511
Advanced lead-acid (Pb)	3659.303	1,301,085	2434.004	15,360,942	340,205.06	292.3126	0.0278577

TABLE 10 Correlation coefficient (R) and model root mean square error (MRMSE) values.

S/N	Exhaust emission component	ECE 15 (urban driving cycle)		EUDC (extra urban driving cycle)		US06 (city mode driving cycle)	
		MRMSE (ppm)	R	MRMSE (ppm)	R	MRMSE (ppm)	R
1	Carbon monoxide (CO)	103.32	0.99	83.63	0.697	2778.5	0.24
2	Carbon dioxide (CO_2),	2907.7	0.02	60.06	0.170	1954.3	0.47
3	Oxides of nitrogen (NO_X)	39,056	0.57	2349.8	0.793	1038.8	0.91
4	Unburned hydrocarbons (THC)	2860.9	0.26	3559.2	0.310	2720.0	0.67

12.6. Possible Applications of the Results

PHEVs offer greater savings in petroleum energy use compared to conventional hybrid electric vehicles (HEVs). Notably, the savings in petroleum energy increase as the annual equal rate (AER) extends, except in scenarios where the marginal grid mix is dominated by oil fuel. Additionally, higher reductions in greenhouse gas (GHG) emissions are observed with increasing AER, unless the marginal grid mix is primarily fueled by coal or oil. PHEVs that utilize biomass-based fuels (such as a blend of 85% ethanol fuel, known as E85, and hydrogen) may not achieve GHG emissions benefits over traditional HEVs if fossil fuels dominate the marginal generation mix. Regarding PM control technology, condensation scrubbers are specifically designed to capture fine PM, which has become a significant pollutant. These systems are intended for use in waste gas streams that contain high levels of PM. Both new and retrofit installations can employ this technology. However, since condensation scrubbing systems are relatively new, they are not widely available for purchase. Emission wave patterns include:

(a). Airflow: Typical airflows are on the order of 10 popular cubic meters per second (m^3/s)

(b). Temperature: The waste gas entering a condensation scrubber is usually cooled to saturation conditions, about 20–26°C (68–78°F)

(c). Pollutant Loading: The effectiveness of the primary PM control technology is determined by its ability to manage different pollutant loadings. Fine PM can sometimes constitute up to 90% of the total mass of PM emissions from a combustion engine, and many primary control technologies have low efficiency in collecting fine PM.

(d). Particular Attention: Cadmium and other heavy metals are often found in the fine fraction of PM emissions from combustion sources. The most effective way to reduce metal emissions may be to use a condensation scrubber to capture PM.

A well-defined technical specification can give suppliers the framework to offer their best solutions. It should also outline any requirements that must be met, which is crucial if we later need to argue that the provided equipment does not meet our specified criteria. If such requirements are not included in the specification, it becomes more difficult to demonstrate that they were essential. It may be beneficial to categorize the technical specifications into “critical” and “desirable” categories.

12.7. Strengths and Limitations of ANFIS

The resilience of the outcomes provided by ANFIS is what makes it fulfilling. ANFIS and other system learning algorithms have specific generalization functionality similar to that of neural networks [25]. ANFIS can take in crisp input, form it into membership functions and fuzzy policies, and then use reasoning to produce crisp output from fuzzy policies once more. Programs with clean inputs and outputs can now be used. It is a very capable tool that has not yet been investigated in many other complex and nonlinear approximation and manipulation problems. ANFIS has a significant computing cost because of its complicated shape and gradient mastery. It represents a significant barrier to applications with large input volumes.

The sort and range of membership capabilities, the position of a membership feature, and the curse of dimensionality are, in general, the limits. Additionally, the trade-off between interpretability and accuracy is seen to be a significant issue.

Within ANFIS, tunable parameters include joining characteristic parameters as well as hence parameters. This requires an effective educational system that can adjust the parameters more successfully. Computational value and parameter complexity are directly correlated. Thus, the higher the ANFIS architecture’s parameters, the higher the computing and educational costs, which is clarified by looking at the Iris class dataset [9]. Here, the genfis1 tool in MATLAB is used to build ANFIS-1, which generates ANFIS using a grid partitioning strategy. ANFIS-2 is the one produced by subtractive clustering using MATLAB’s genfis2 tool. Additionally, ANFIS-3 is the network shape produced by the MATLAB genfis3 program utilizing the fuzzy c-imply clustering algorithm.

12.8. Formatting and Typographical Errors

For the specific training of an ANFIS network, a hybrid learning rule is proposed that combines the gradient descent approach with the least-squares estimator (LSE). As a supervised learning method, it requires a teaching signal, which can be challenging to provide when the ANFIS network functions as a control system, since the desired control actions that the teaching signal represents are often unknown. Various ANFIS learning techniques have been proposed in the literature, particularly when ANFIS is implemented as a MIMO (Multiple Input Multiple Output) controller. For example, one method utilizes a unique ANFIS learning approach known as temporal back-propagation (TBP). This approach controls a nonlinear MIMO system by considering both the controller and the plant as a single unit at each step. However, this method is quite complex and computationally intensive.

- An ANFIS controller design method for temperature control in plastic extrusion device at exclusive set factor changes in addition to unexpected input disturbances controlled with one-of-a-kind control strategies. The temperature of the plastic extrusion machine has a huge range of variant concerns to diverse disturbances. The machine is usually nonlinear and so controlling the temperature is a tedious manner, because it has a couple of ranges and the system is coupled with each other. The plastic extrusion manner uses first-order transfer function. The four manipulate strategies are traditionally PI, PID, and sensible controllers, fuzzy and ANFIS. The tuning synchronizes the controller to the managed variable and make the system to paintings at its preferred running condition. All four control techniques simulate the use of MATLAB/Simulink. It has been concluded that ANFIS controller offers higher performance than the other three controllers
- An ANFIS controller layout technique for temperature control in plastic extrusion system at one-of-a-kind set factor adjustments in addition to unexpected input disturbances controlled with special control techniques. The temperature of the plastic extrusion device has a huge range of version issues to diverse disturbances. The gadget is commonly nonlinear, and so controlling the temperature is a tedious procedure, because it has more than one level and the system is coupled with other different systems. The plastic extrusion process makes use of first-order switch feature. The four control strategies are traditionally PI, PID, and two smart controllers, fuzzy and ANFIS. The tuning synchronizes the controller to the controlled variable and make the procedure to paintings at its desired operating circumstance. All four4 control methods simulate the usage of MATLAB/Simulink. It has been concluded that ANFIS controller offers better overall performance than the other three controllers

12.9. ANFIS Controller Performance

This research segment centers on assessing the performance capabilities of the ANFIS controller. Specifically, the focus is on evaluating its aptitude to forecast the values of various vehicle exhaust emission constituents—including CO, CO_2, NOx, and THC. This assessment follows the learning process outlined in the ANFIS control strategy, as per Equation 6. The simulation results, encompassing the ANFIS controller's performance metrics, are detailed in Table 11.

12.10. Technical Suggestions

A detailed exploration of the key elements of sensitivity analyses inclusive of a detailed exploration of the important thing components of sensitivity analyses, which includes: (1) what sensitivity analyses are, why they're needed, and the way frequently they're utilized in practice; (2) the exclusive types of sensitivity analyses that one can do, with examples from the literature; (3) some often requested questions on sensitivity analyses; and (4) some tips on how to report the consequences of sensitivity analyses in clinical trials.

Under ECE 15 (urban driving cycle) conditions, the ANFIS exhibits an efficiency of 43.49% for CO, with a corresponding CRMSE of 1863.6 ppm. In contrast, EUDC yields a higher efficiency of 66.66%, yet a CRMSE of 1664.3 ppm. Regarding CO_2, the ANFIS achieves an efficiency of 9.092% and a CRMSE of 1.2786 ppm under ECE 15 (urban

TABLE 11 Controller effectiveness (Eff, %) and controlled root mean square error (CRMSE) values.

S/N	Exhaust emission component	ECE 15 (urban driving cycle)		EUDC (extra urban driving cycle)		US06 (city mode driving cycle)	
		CRMSE (ppm)	EFF (%)	CRMSE, ppm	EFF (%)	CRMSE (ppm)	EFF (%)
1	Carbon monoxide (CO)	1863.6	43.49	1664.3	66.66	1863.6	43.49
2	Carbon dioxide (CO_2)	1.2786	9.092	0.6627	4.761	1.0493	7.411
3	Oxides of nitrogen (NO_x)	605.35	66.66	1103.4	66.66	873.07	66.66
4	Unburned hydrocarbons (THC)	22.945	33.33	31.634	33.33	28.163	33.33

driving cycle). For intermittent and sequential fuel injection, the efficiencies and CRMSEs vary widely—0.170 and 60.06 ppm, and 0.47 and 1954.3 ppm, respectively. In the realm of NOx, EUDC fuel injection results in a 66.66% efficiency and a CRMSE of 605.35 ppm, while intermittent and US06 (city mode driving cycle) yield similar efficiencies of 66.66% but differing CRMSEs of 1103.4 ppm and 873.07 ppm. For THC, the ANFIS effectiveness is consistently 33.33%, accompanied by CRMSEs of 22.945 ppm, 31.634 ppm, and 28.163 ppm under continuous, intermittent, and sequential fuel injection, respectively.

The ANFIS controller can be effectively employed by integrating the BOOST platform with the MATLAB/Simulink platform through a MATLAB API interface element.

13. Conclusions

1. This article explains the Ecoscore environmental rating system's approach. The environmental rating system for road cars, Ecoscore, has been given a thorough and transparent overview. With the help of this approach, vehicles with various drivetrains and fuel types can be evaluated. To show how this methodology can be used, actual vehicle outcomes were calculated and discussed. According to the research done using the Ecoscore methodology, the environmental performance of cars has improved over time. The job also entails creating a vehicle that runs primarily on batteries and has extremely low energy consumption, pollution, and noise levels, as well as a competitive purchase price, a long driving range, and acceptable performance.
2. It is praiseworthy that efforts are being made to reduce vehicle exhaust emissions in order to improve air quality. When compared to fossil fuel-powered vehicles, electric cars are frequently pushed as a more environmentally friendly form of transportation. Many electric cars, on the other hand, also require some power from the electrical grid in order to function. While producing electricity, a sizeable part of the electric grid emits a significant amount of greenhouse gases. The GHG emissions from both electric and fossil fuel-powered cars were taken into account in this study to assess potential areas for development in the two designs. The outcome showed that electric cars are not always superior to fossil fuel-powered vehicles in terms of the associated GHG emissions from the electricity grid.
3. The IVE model was used to predict emissions in order to differentiate between the effects of different driving styles on vehicular exhaust emissions. Figure 8 contrasts various contaminants' emission rates calculated using the IVE model for various driving styles. It is evident that release.
4. Passenger car exhaust emissions of CO_2 are an enormous and increasing aspect of weather exchange. The proportion of EVs in passenger automobile fleets could be multiplied to useful resources inside the reduction of those emissions; however, this is based on the fuel blend used to supply the electricity that powers EVs. For an expansion of internal combustion engine vehicles (ICEVs) and hybrid electric vehicles, this research compares and analyses the records on indirect emissions (HEVs). The evaluation additionally compares the well-to-wheels emissions of the contemporary passenger vehicle fleets in each state to a fictitious EV fleet with the typical electricity generation needs of the three EVs under consideration.
5. An overview of the ANFIS structure has been provided on this research project, allowing you to concentrate on the network's computational complexity. The quantity of parameters and policies has a significant impact on how ANFIS-based absolute fashions are computed. Furthermore, the interpretability of rules, parameter education, and the curse of dimensionality are distinct challenges that must be overcome in order to apply solutions for problems involving large, complex input styles. For this reason, ANFIS is frequently combined with additional input selection, rule discounting, and parameter tweaking techniques, which further raises the complexity of the model's architecture.
6. There may be enough space for improvement in the ANFIS structure, despite the numerous structural and parameter optimization methodologies that have been put out in the literature, to enable programs in large issues to be completed without issue. In order to overcome those issues, conceptual ideas based on this study have been put forth, which resemble exciting recommendations for future research.
7. Twin gasoline engines are used in recent times to triumph over the shortage of fossil fuels and fulfill stringent exhaust fuel emission policies. They have several advantages over conventional diesel engines; this article makes use of experimental effects obtained from a dual gasoline engine for developing fashions to expect performance and emission parameters. Conventional modeling efforts to understand the relationships between the input and the output variables require thermodynamic analysis that's complex and time-consuming. As an end result, efforts had been made to apply synthetic intelligence modeling strategies like fuzzy good judgement, synthetic neural community (ANN), genetic algorithm (GA), and the like. This article makes use of a neuro-

fuzzy modeling technique, ANFIS for growing prediction fashions for performance and emission parameter of a twin gasoline engine. Percentage load, percent liquefied petroleum gasoline (LPG), and injection timing (IT) had been used as input parameters, whereas output parameters include BSEC, BTE, exhaust gasoline temperature (EGT), and smoke. So, one can in addition improve the prediction accuracy of the model, GA has been used to optimize ANFIS. GA-optimized ANFIS gives higher prediction accuracy of more than 90% for all parameters except for smoke, in which there's a sizeable development from 46.67% to 73.33%, while in comparison to conventional ANFIS version

Funding Information

Support by Science and Technology Development Fund (STDF), Egypt, through the awarded grant No. ID 41580, on "Air Pollution: Vehicles Exhaust".

Conflict of Interest

On behalf of all the authors, the corresponding author states that there is no conflict of interest.

Availability of Data and Materials

The data and materials that support the findings of this study are available from the corresponding author upon reasonable request.

Acknowledgements

The authors acknowledge the support of Science and Technology Development Fund (STDF), Egypt, through the awarded grant No. ID 41580, on "Air Pollution: Vehicles Exhaust". The authors would like to thank University of Helwan, which made this study possible.

Contact Information

Mohamed Salah El Din Shiba, corresponding author
mohamed.shiba@hti.edu.eg; melhamed@msa.edu.eg

References

1. Essien, E., Ibrahim, H., Mehrandezh, M., and Idem, R., "Adaptive Neuro-Fuzzy Inference System (ANFIS)–Based Model Predictive Control (MPC) for Carbon Dioxide Reforming of Methane (CDRM) in a Plug Flow Tubular Reactor for Hydrogen Production," *Thermal Science and Engineering Progress* 9 (2019): 148-161, doi:https://doi.org/10.1016/j.tsep.2018.11.010.
2. Searchinger, T., Heimlich, R., Houghton, R.A., Dong, F. et al., "Use of US Croplands for Biofuels Increases Greenhouse Gases through Emissions from Land-Use Change," *Science* 319, no. 5867 (2008): 1238-1240, doi:https://doi.org/10.1126/science.1151861.
3. Kolarova, V., Anderson, J.E., and Hardinghaus, M., "Indirect CO_2 Emissions of Electric Vehicles: Insights from Real-World Vehicle Use," in *Conference: Transport Research Arena 2018*, Vienna, Austria, 2018.
4. Arvesen, A., Luderer, G., Peh, M., Bodirsky, B.L. et al., "Deriving Life Cycle Assessment Coefficients for Application in Integrated Assessment Modelling," *Environmental Modelling & Software* 99 (2018): 111-125, doi:https://doi.org/10.1016/j.envsoft.2017.09.010.
5. Märtz, A., Plötz, P., and Jochem, P., "Global Perspective on CO_2 Emissions of Electric Vehicles," *Environ. Res. Lett.* 16 (2021): 054043, doi:https://doi.org/10.1088/1748-9326/abf8e1,3.
6. Edelenbosch, O.Y., Hob, A.F., Nykvist, B., Girod, B. et al., "Transport Electrification: The Effect of Recent Battery Cost Reduction on Future Emission Scenarios," *Climatic Change* 151 (2018): 95-108, doi:https://doi.org/10.1007/s10584-018-2250-y.
7. Wolfram, P., Weber, S., Gillingham, K., and Hertwich, E.G., "Pricing Indirect Emissions Accelerates Low—Carbon Transition of US Light Vehicle Sector," *Nature Communications* 12 (2021): 7121, doi:https://doi.org/10.1038/s41467-021-27247-y.
8. Marmiroli, B., Messagie, M., Dotelli, G., and Van Mierlo, J., "Electricity Generation in LCA of Electric Vehicles: A Review," *Applied Sciences* 8, no. 8 (2018): 1384, doi:https://doi.org/10.3390/app8081384.
9. Hassouna, F.M.A., Nassar, R., and Tubaleh, H., "Electric Vehicles as an Alternative to Conventional Vehicles: A Review," *Smart Cities* 4, no. 1 (2021): 372-404, doi:https://doi.org/10.3390/smartcities4010022.
10. O'Donoghue, C., Chyzheuskaya, A., Grealis, E., Finnegan, W. et al., "Measuring GHG Emissions Across the Agri-Food Sector Value Chain: The Development of a Bio-Economy Input/Output Model," in *Proceedings in System Dynamics and Innovation in Food Networks*, Garmisch-Partenkirchen, Germany, 2018, 38-69, doi:https://doi.org/10.18461/pfsd.2018.1803.
11. Märtz, A., Plötz, P., and Jochem, P., "Global Perspective on CO_2 Emissions of Electric Vehicles," *Environmental Research Letters* 16, no. 5 (2021): 054043, doi:https://doi.org/10.1088/1748-9326/abf8e1.

12. Wong, E.Y.C., Ho, D.C.K., So, S., Tsang, C.-W. et al., "Life Cycle Assessment of Electric\Vehicles and Hydrogen Fuel Cell Vehicles Using the GREET Model—A Comparative Study," *Sustainability* 13 (2021): 4872, doi:https://doi.org/10.3390/su13094872.
13. Pereirinha, P.G., Gonzálezd, M., Carrilerod, I., Anseánd, D. et al., "Main Trends and Challenges in Road Transportation Electrification," *Transportation Research Procedia* 33 (2018): 235-242.
14. Dillman, K.J., Árnadóttir, Á., Heinonen, J., Czepkiewicz, M. et al., "Review and Meta-Analysis of EVs: Embodied Emissions and Environmental Break Even," *Sustainability* 12 (2020): 9390, doi:https://doi.org/10.3390/su12229390.
15. Al-Buenain, A., Al-Muhannadi, S., Falamarzi, M., Kutty, A.A. et al., "The Adoption of Electric Vehicles in Qatar Can Contribute to Net Carbon Emission Reduction but Requires Strong Government Incentives," *Vehicles* 3 (2021): 618-635, doi:https://doi.org/10.3390/vehicles3030037.
16. Bayani, R., Soofi, A.F., Waseem, M., and Manshadi, S.D., "Impact of Transportation Electrification on the Electricity Grid—A Review," *Vehicles* 4 (2022): 1042-1079, doi:https://doi.org/10.3390/vehicles4040056.
17. Caro, D., Bastianoni, S., Borghesi, S., and Pulsellia, F.M., "On the Feasibility of a Consumer-Based Allocation Method in National GHG Inventories," *Ecological Indicators* 36, no. 2014 (2014): 640-643, doi:https://doi.org/10.1016/j.ecolind.2013.09.021.
18. Sobol, Ł. and Dyjakon, A., "The Influence of Power Sources for Charging the Batteries of Electric Cars on CO_2 Emissions during Daily Driving: A Case Study from Poland," *Energies* 13 (2020): 4267, doi:https://doi.org/10.3390/en13164267.
19. Lynas, M., Houlton, B.Z., and Perry, S., "Greater Than 99% Consensus on Human Caused Climate Change in the Peer-Reviewed Scientific Literature," *Environmental Research Letters* 16 (2021): 114005, doi:https://doi.org/10.1088/1748-9326/ac2966.
20. Thompson, D.J., "The Drive-by Test," in *N3: Automotive Engineering II* Lecture Notes, (Southampton, UK: University of Southampton, 2002), https://doi.org/10.18461/pfsd.2018.180
21. Adegbohun, F., Von Jouanne, A., Phillips, B., Agamloh, E. et al., "High Performance Electric Vehicle Powertrain Modeling, Simulation and Validation," *Energies* 14, no. 5 (2021): 1493, doi:https://doi.org/10.3390/en14051493.
22. Joumard, R., Philippe, F., and Vidon, R., "Reliability of the Current Models of Instantaneous Pollutant Emissions," *The Science of the Total Environment* 235 (1999): 133-142, doi:http://dx.doi.org/10.1016/S0048-9697(99)00202-8.
23. Choudhury, M., Rao, A.R., and Vadawale, S.V., "Correlated Radio: X Ray Emission in the Hard States of Galactic Microquasars," *The Astrophysical Journal* 593 (2002): 452-462.
24. Miller, P. and Kumar, A., "Development of Emission Parameters and Net Energy Ratio for Renewable Diesel from Canola and Camelina," *Energy* 58 (2013): 426-437, doi:https://doi.org/10.1016/j.energy.2013.05.027.
25. Pérez-Martínez, P.J., Miranda, R.M., Nogueira, T., Guardani, M.L. et al., "Emission Factors of Air Pollutants from Vehicles Measured Inside Road Tunnels in São Paulo: Case Study Comparison," *Int. J. Environ. Sci. Technol.* 11 (2014): 2155-2168, doi:https://doi.org/10.1007/s13762-014-0562-7.
26. Takagi, T. and Sugeno, M., "Derivation of Fuzzy Control Rules from Human Operator's Control Actions," *IFAC Proceedings Volumes* 16, no. 13 (1983): 55-60, doi:https://doi.org/10.1016/S1474-6670(17)62005-6.
27. Abouel-Seoud, S.A., Shiba, M.S., and Abdallah, A.S., "Real World Evaluation and Control of Vehicle Engine Exhaust Air Pollution Using Adaptive Neural Fuzzy Inference System," *International Journal of Engine Research* 24, no. 5 (2023): 2233-2250, doi:https://doi.org/10.1177/14680874221133213.
28. Yamasaki, Y., Ikemura, R., and Kaneko, S., "Model-Based Control of Diesel Engines with Multiple Fuel Injections," *Int. J. Engine Res.* 19, no. 2 (2018): 257-265, doi:https://doi.org/10.1177/1468087417747738.
29. Martins, M. and Zhao, H., "Performance and Emissions of a 4-Cylinder Gasoline Engine with Controlled Auto-Ignition," *J. Braz. Soc. Mech. Sci. Eng.* 34, no. 4 (2012): 436-440, doi:https://doi.org/10.1590/S1678-58782012000400003.
30. Kim, G., Moon, S., Lee, S., and Min, K., "Numerical Analysis of the Combustion and Emission Characteristics of Diesel Engines with Multiple Injection Strategies Using a Modified 2-D Flamelet Model," *Energies* 10 (2017): 1292, doi:https://doi.org/10.3390/EN10091292.